UWB CONFORMAL ANTENNAS

B. Kramer, M. Lee, C.-C. Chen, G. Kiziltas, J. L. Volakis and J. H. Holloran

The Ohio State University

ElectroScience Laboratory

Department of Electrical Engineering
1320 Kinnear Road
Columbus, Ohio 43212

20040804 059

5027272-101

REPORT DOCUMENTATION PAGE	1. REPORT NO.	2.	3. Recipient's Accession No.
4. Title and Subtitle **UWB CONFORMAL ANTENNAS**			**5. Report Date** July 2004
			6.
7. Author(s) B. Kramer, M. Lee, C.-C. Chen, G. Kiziltas, J. L. Volakis, J. H. Holloran			**8. Performing Org. Rept. No.** 744504-2
9. Performing Organization Name and Address The Ohio State University ElectroScience Laboratory 1320 Kinnear Road Columbus, OH 43212			**10. Project/Task/Work Unit No.**
			11. Contract (C) or Grant (G) No. (C) N00014-03-C-0229
12. Sponsoring Organization Name and Address John Moniz, Program Officer Expeditionary Warfare C4ISR S&T, ONR 353 Office of Naval Research Ballston Center Tower One 800 North Quincy Street Arlington, VA 22217-5660			**13. Report Type/Period Covered** Annual Technical Report
			14.

15. Supplementary Notes

16. Abstract (Limit: 200 words)

Antennas currently used for VHF and UHF band operation (30-512MHz) are bulky and often inefficient. Antenna miniaturization techniques can be employed to reduce their size and improve performance. The two most common approaches are the use of dielectric material or reactive (inductive and capacitive) loading to create a slow wave structure by reducing the effective wavelength in the antenna structure. In this report the concept of miniaturizing a broadband spiral antenna using dielectric materials is experimentally demonstrated using 2" and 6" diameter spirals and further investigated using simulations. Additionally, an approach using lumped inductors and capacitors for miniaturization is also investigated. It is shown that the effectiveness of dielectric loading and reactive loading is limited by their ability to practically load the near field region of the antenna. Using such loading techniques, a miniaturization factor of nearly 2 was achieved. However, this is insufficient for operation down to 30MHz using a 6" or 15" aperture. To achieve operation down to 30 MHz using a 6" or 15" aperture, miniaturization factors of 11 and 4.5 are necessary. To increase the miniaturization and overcome these limitations, methods are introduced that will allow for the antenna fields to be confined closer to the antenna so that they can be loaded more effectively using practical loading geometries.

17. Document Analysis

a. Descriptors

b. Identifiers/Open-Ended Terms

c. COSATI Field/Group

18. Availability Statement	19. Security Class (This report) Unclassified	21. No. of Pages 75
Approved for public release; Distribution is unlimited.	20. Security Class (This page) Unclassified	22. Price

(See ANSI-Z39.18)　　　　　*See Instructions on Reverse*　　　　　OPTIONAL FORM 272(4-77)
Department of Commerce

UWB CONFORMAL ANTENNAS

B. Kramer, M. Lee, C.-C. Chen, G. Kiziltas, J. L. Volakis and J. H. Holloran

Annual Technical Report 744504-2
Contract No. N00014-03-C-0229
July 2004

5027272-101

REPORT DOCUMENTATION PAGE	1. REPORT NO.	2.	3. Recipient's Accession No.
4. Title and Subtitle **UWB CONFORMAL ANTENNAS**			**5. Report Date** July 2004
			6.
7. Author(s) B. Kramer, M. Lee, C.-C. Chen, G. Kiziltas, J. L. Volakis, J. H. Holloran			**8. Performing Org. Rept. No.** 744504-2
9. Performing Organization Name and Address The Ohio State University ElectroScience Laboratory 1320 Kinnear Road Columbus, OH 43212			**10. Project/Task/Work Unit No.**
			11. Contract (C) or Grant (G) No. (C) N00014-03-C-0229
12. Sponsoring Organization Name and Address John Moniz, Program Officer Expeditionary Warfare C4ISR S&T, ONR 353 Office of Naval Research Ballston Center Tower One 800 North Quincy Street Arlington, VA 22217-5660			**13. Report Type/Period Covered** Annual Technical Report
			14.

15. Supplementary Notes

16. Abstract (Limit: 200 words)

Antennas currently used for VHF and UHF band operation (30-512MHz) are bulky and often inefficient. Antenna miniaturization techniques can be employed to reduce their size and improve performance. The two most common approaches are the use of dielectric material or reactive (inductive and capacitive) loading to create a slow wave structure by reducing the effective wavelength in the antenna structure. In this report the concept of miniaturizing a broadband spiral antenna using dielectric materials is experimentally demonstrated using 2" and 6" diameter spirals and further investigated using simulations. Additionally, an approach using lumped inductors and capacitors for miniaturization is also investigated. It is shown that the effectiveness of dielectric loading and reactive loading is limited by their ability to practically load the near field region of the antenna. Using such loading techniques, a miniaturization factor of nearly 2 was achieved. However, this is insufficient for operation down to 30MHz using a 6" or 15" aperture. To achieve operation down to 30 MHz using a 6" or 15" aperture, miniaturization factors of 11 and 4.5 are necessary. To increase the miniaturization and overcome these limitations, methods are introduced that will allow for the antenna fields to be confined closer to the antenna so that they can be loaded more effectively using practical loading geometries.

17. Document Analysis

a. Descriptors

b. Identifiers/Open-Ended Terms

c. COSATI Field/Group

18. Availability Statement	19. Security Class (This report) Unclassified	21. No. of Pages 75
Approved for public release; Distribution is unlimited.	20. Security Class (This page) Unclassified	22. Price

(See ANSI-Z39.18)   *See Instructions on Reverse*   OPTIONAL FORM 272(4-77)
 Department of Commerce

Table of Contents

List of Figures

Chapter 1

Executive Summary

The goal of this research is to address the existing need of replacing bulky and often inefficient antennas currently used for VHF and UHF band operation (30-512MHz) with particular emphasis on the lower 30-88MHz band. The target antenna size is no larger than 15 inches in diameter but our goal is for a 6" aperture. This is to be achieved by using high contrast meta-material substrates/superstrate to increase the electrical size of the antenna and by using the state-of-art optimization procedure for optimizing the meta-material profile to provide the optimal radiation performance. The objectives of the current task includes (1) validating the performance of a square spiral antenna predicted from previous work obtained from 6-inch spiral antenna prototypes; (2) demonstrating antenna miniaturization using uniform LTCC substrates; (3) developing baseline antenna prototypes loaded with high contrast meta-material superstrate/substrate.

Objective (1) was achieved by measuring and improving the square slot spiral antenna design. The significant design improvements include (a) a better slot-line termination which improves axial ratio and efficiency at lower frequencies; (b) utilization of a broadband balun to feed the antenna reduces gain measurement error caused by cable radiation; (c) a lossless cavity mode suppression technique that improves gain at upper frequencies. Objective (2) was achieved experimentally and numerically by using a 2" square slot spiral antenna treated with uniform dielectric superstrate (see Figure 1.1). Table 1.1 summarizes the initial experimental results for lowering the -15dB gain point by loading the 2" antenna with various high-contrast superstrates for different dielectric constants and thicknesses. Note that the frequency for the -15 dB gain point without material loading is at 895 MHz. However, with a 3mm (ε_r= 90) dielectric superstrate this point was brought down to 598 MHz corresponding to a miniaturization factor (MF) of approximately 1.5.

ε_r	t/λ_g	Frequency with -15dBi Gain, f_L	MF=f_0/f_L	% Reduction
37	0.038	763 MHz	1.172	14.7
90	0.059	633 MHz	1.414	29.3
90	0.089	598 MHz	1.497	33.2

Table 1.1 2" square spiral summary for the frequency shift of the -15dBi gain point.
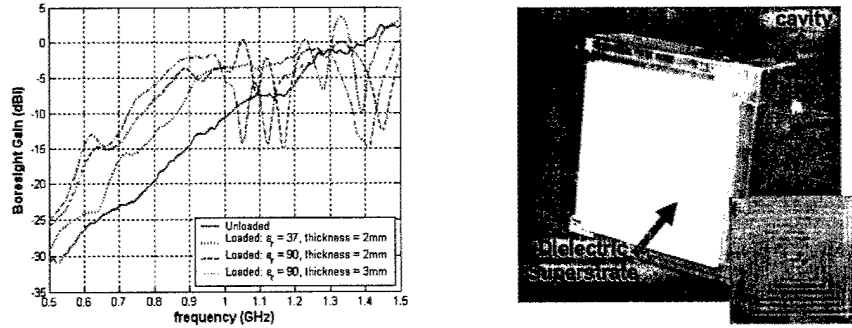
Figure 1.1 Cavity Backed 2" Square Slot Spiral Loaded with a Dielectric (LTCC) Superstrate.

To verify that the miniaturization behavior observed in the 2"x2" prototype scales to larger apertures, a 6"x6" square spiral antenna prototype was fabricated and measured with/without a high-dielectric superstrate. The results confirmed the performance predicted from the 2" predecessor and that our LTCC loading is scalable. That is, the measured 6" aperture data compared well with the 2" scaled gain data. The superstrate used to load the 6" prototype had a dielectric constant of 30 and a thickness of 0.25".

To fully investigate the miniaturization of the spiral antenna, simulations were carried out using the finite element method. It was found that any MF is achievable as long as the reactive near field region of the antenna is sufficiently loaded by the dielectric material. However, the amount of material required to do so is impractical to implement because the width of the dielectric slab needs to be much larger than the diameter of the spiral. That is, the MF was limited only by practical loading considerations such as width, profile (thickness), dielectric constant, weight and so forth. Using such practical loading profiles, we were able to achieve a MF of up to 1.8 as shown in Figure 1.2 (lower dashed line). However, maximum utilization of the dielectric loading can allow for up to a factor of 10 (see solid curve) in miniaturization when using ε_r=100. Further, it is known that to achieve operation down to 30 MHz using a 6" or 15" aperture, miniaturization factors of 11 and 4.5 are required respectively. To realize such reductions other approaches were explored such as reactive loading and a more high risk

8

approach using formal design optimization procedures. That is, additional and significant miniaturization can be achieved but only through other design approaches thus considered so far.
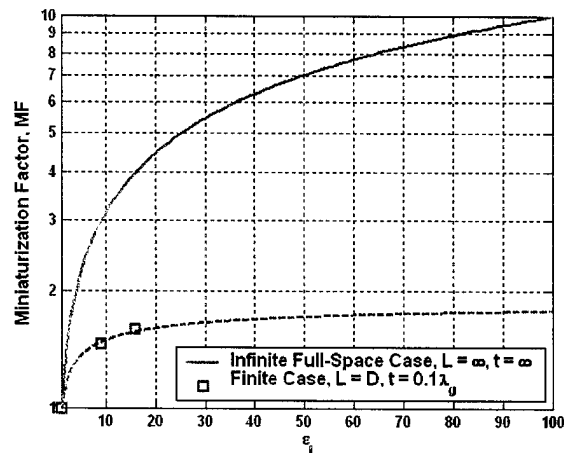
Figure 1.2 Miniaturization factor as a function of dielectric constant.

The reactive loading approach was pursued using lumped inductive and capacitive elements to create a slow wave antenna structure. It was found that this method was very effective in reducing the wavelength of the guided wave within the spiral geometry. However, this did not directly translate into a corresponding increase in gain at low frequencies as expected. It was observed that for a designed wavelength reduction factor of 3.3 only a MF of 1.2 was achieved in terms of gain. We suspect that this is likely due to the 2D nature of the LC loading whereas the 3D antenna fields require volumetric loading.

Our previous efforts using formal design optimization procedures indicate that properly designed dielectrics or a combination of different materials can lead to designs which have greater bandwidth and small size for narrowband antennas. Here, this approach was extended to broadband antenna design by designing from scratch a 6" antenna for UHF operation (230-330MHz). The initial results obtained from optimizing the metallization and material topology led to a flat -4 to -5dB return loss response over the entire 30% bandwidth. This was a significant improvement over the initial design, which only had a -4dB response over a small fraction of the desired bandwidth. Though the obtained return loss behavior does not satisfy the antenna requirements, the promising initial trials and the confidence obtained in the design methodology was a significant step and will be pursued vigorously in the future for the section of the antenna operating in the low frequency region.

9
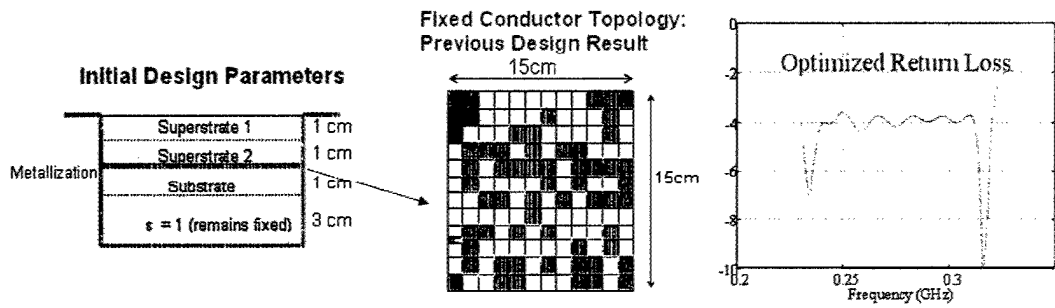
Figure 1.3 Example of volumetric design optimization for UHF antenna (230-330MHz).

In summary, our studies on miniaturization either by dielectric loading or reactive L/C loading allows us to conclude that wavelength miniaturization can be effectively achieved and predicted. However, this wavelength reduction does not translate to a corresponding shift of the gain curve towards lower frequencies. It is our belief that this is due to the 3D nature of the radiated fields around the antenna which must be loaded sufficiently to achieve greater reductions. To realize the reductions required for operation down to VHF frequencies, we must investigate more complex loading profiles and three dimensional antenna designs that will allow for more effective loading of the antenna fields. The concept is to confine the fields closer to the antenna so that they can be loaded more effectively using practical material dimensions. One approach that will be pursued in the next few months is to use the material shape and a varying dielectric constant to reshape the fields of the antenna much like a lens (see Figure 1.4). Being able to reshape the fields would allow confinement of the fields closer to the antenna. Another approach is to address the issue of the low frequency fields extending outside the diameter by using a non-planar shape. The concept is to alter the planar spiral shape such that low frequency fields can be confined closer to the antenna aperture without negatively impacting the performance (see Figure 1.5). This is illustrated in Figure 1.5 and follows the proposed concept of full volume design of the dielectric and metallization of the antenna.
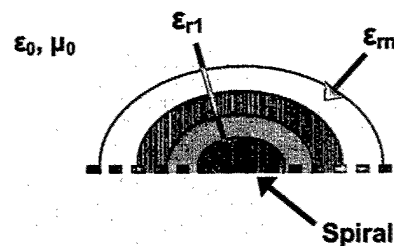
Figure 1.4 Material profile concept for improved miniaturization.

10

Metallization (slot spiral or other slot and printed elements)

Capacitive loading

Inductive meandering

LD crystals or other meta-materials and graded dielectrics, embedded FSS structures

ε_0, μ_0
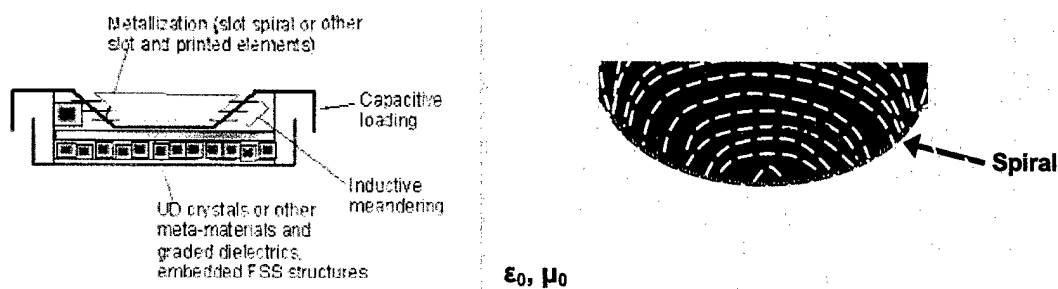
Spiral

Figure 1.5 Illustration of the 3D spiral design concept for improved miniaturization. Left: Originally proposed design. Right: Currently pursued design.

In conclusion, our simple planar material loading of the spiral antenna allowed for a nearly factor of 2 in miniaturization and this was demonstrated with measurements and simulations. For further miniaturization and to take better advantage of lumped element loading as well as material loading, we plan to pursue volumetric design in accordance with the specific ideas outlines in this report.

Chapter 2

Introduction

2.1 Objective

The goal of this research is to address the existing need of replacing bulky and often inefficient antennas currently used for VHF and UHF band operation (30-512MHz) with particular emphasis on the lower 30-88MHz band. This effort focuses on developing a small antenna capable of operating with all waveforms between 30 MHz and 512 MHz (VHF/UHF) which would include:

SINCGARS	30-88 MHz	V-pol
VHF AM	117-176 MHz	V-pol
UHF LOS COMS	225-400 MHz	V-pol
HAVE QUICK	225-400 MHz	V-pol
UHF SATCOM	240-320 MHz	RHCP
EPLRS	450-470 MHz	V-pol

The target antenna size is no larger than 15 inches in diameter but our goal is for a 6" aperture. This is to be achieved by using high contrast meta-material substrates/superstrate to increase the electrical size of the antenna and by using the state-of-art optimization procedure for optimizing the meta-material profile to provide optimal radiation performance. The objectives of the current task includes (1) validating the performance of a square spiral antenna predicted from previous work obtained from 6-inch spiral antenna prototypes; (2) demonstrating antenna miniaturization using uniform LTCC substrates; (3) developing baseline antenna prototypes loaded with high contrast meta-material superstrate/substrate.

2.2 Technology Description

2.2.1 UWB Slot Spiral Antenna

The spiral antenna is currently used in a variety of applications that require a conformal broadband circularly polarized antenna. The spiral antenna's planar structure makes is well suited for conformal mounting and it is easily capable of achieving a 9:1 bandwidth which makes it very attractive for broadband applications. In addition, for a given operational frequency f_0, the aperture of a spiral antenna is a factor of π smaller than that of a dipole which makes it a compact design. A spiral antenna without a backing cavity would radiate equally well to the front or back side. However, improved directivity and unidirectional radiation can be achieved through the use of a cavity or ground plane. Currently, most spiral antennas that appear in the literature are circular spirals that are of wire or microstrip type. However, it has been shown that the square slot spiral has many advantages over the circular configuration and wire type spirals. The first advantage is that for a given frequency, f_0, the resonant band on a square spiral will occur at a radius that is up to 22% smaller than a circular spiral. That is, for a given aperture size the square spiral can operate down to lower frequencies. The second reason is that the slot design is a more efficient radiator than the wire type design due to reduced losses since the fields are confined within the slot. This also leads to less energy dissipation in the arm termination, a more uniform pattern and better polarization purity (cross-polarization).
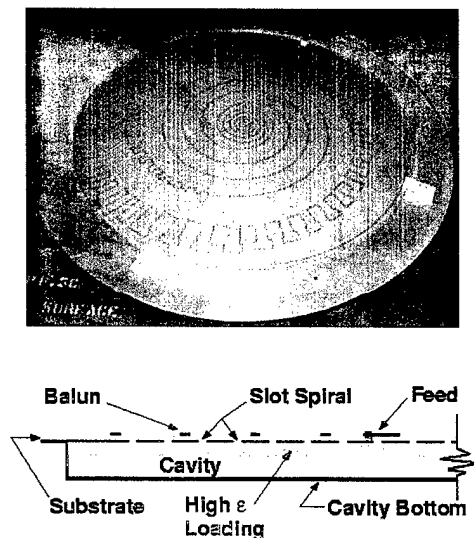
Figure 2.1 Cavity Backed 18" Circular Slot Spiral.

2.2.2 Antenna Miniaturization using Materials

The purpose of antenna miniaturization is to make the antenna operate at lower frequencies by effectively increasing its electrical size but not its physical size. That is, an antenna, which is typically too small to operate at a given frequency, can do so if it is properly loaded with materials. Miniaturization using high-contrast materials can be explained by showing the propagation velocity of currents along the antenna arms. Essentially, loading the antenna with material slows down the current's propagation on the antenna by reducing the effective wavelength in the antenna structure. Therefore, the phase variation along the antenna arm becomes faster. This makes the antenna appear electrically larger than it physically is and, as a result, the initial operating frequency of the antenna is lowered.

There are other approaches that can be used to miniaturize an antenna such as reactive loading. However, material loading has a distinct advantage which is that it allows the loading of the antenna fields using a volume of space. Magnetic material can be used in conjunction with dielectric material for improved impedance matching and miniaturization, but the disadvantage is that available magnetic materials are narrowband and require a biasing field to limit losses. Thus, for broadband antenna designs, one is limited to using dielectrics only.

2.3 Technical Issues

2.3.1 Antenna Design

The presence of high-contrast material affects the radiation characteristics significantly by changing the impedance, bandwidth and radiation patterns. Leaky waves and surface waves can also be introduced when high-contrast or thick loading is used. Using a high-contrast material loading without paying attention to such tradeoffs and not using proper antenna design modifications could result in disappointing performance due to the adverse effects introduced by the material. Physical constraints that require a low-profile antenna makes it even more challenging to reach an optimal tradeoff design.

The termination of the spiral arms ultimately determines the trade-off between the radiation efficiency and axial ratio/cross-polarization. Resistive terminations are necessary to reduce currents reflected from the end of the spiral arms, which in turn improves bandwidth and polarization at the expense of antenna efficiency. Material loading of the spiral naturally leads to

14

stronger currents reaching the end of the spiral arms and therefore a reduction in efficiency. Therefore, proper antenna design and material loading topology must be investigated to address this issue.

A good impedance matching scheme is also important for a miniaturized ultra-wide band (UWB) antenna. The impedance is approximately a constant real number above the first resonance and becomes mainly inductive (e.g. slot spiral) or capacitive (e.g. wire spiral) at low frequencies. Without a proper matching network design, most of the power from the transmitting source will be reflected back to the source from the antenna input terminal even though the antenna itself should be capable of a higher gain (Note that the gain is defined with respect to the power "accepted" by the antenna.). A small UWB balun design is another challenge for feeding a UWB miniaturized antenna. Such a balun must be able to operate over a wide range of frequencies to prevent squinted patterns and must not create unwanted radiation at low frequencies. Small broadband transformer baluns are available from DC to 700 MHz. A special design is needed to extend the upper frequency beyond 1 GHz.

2.3.2 Loading Scheme

This is an important trade-off between miniaturization and practical considerations (cost, size, weight, etc.) and needs to be investigated further. The optimal selection of *type*, *composition* and *shape* of the loading material also needs to be determined. Although, the idea of using a dielectric loading to lower the antenna's operating frequency has existed for a long time, it usually involved low dielectric constant and a homogeneous layer. The lack of proper material and efficient optimization tools were obvious limitations. Most conventional high dielectric materials are ceramics that require high firing temperature and are difficult to machine after being fired. This makes it difficult to design a special dielectric profile required for UWB and high-dielectric antenna designs. For instance, the resonance region on a spiral antenna at different frequencies varies spatially. As the operational frequency decreases, the "resonant ring" moves outward away from the center. This suggests that a dielectric constant of the superstrate should be a function of distance from the center and should increase as the distance increases from the center. Such an approach is desirable for many reasons such as cost, weight, impedance, etc.

15

2.4 Technical Approach

To achieve the maximal miniaturization and antenna performance, the baseline performance of the previous state-of-art square spiral antenna design was revalidated analytically and experimentally. Careful design study and improvements were conducted to further enhance the antenna's performance before applying the high-contrast material treatment, with specific emphasis at low frequencies. Low loss, high-contrast dielectric loadings with simple dielectric profiles were then added to the antenna to demonstrate the concept of antenna miniaturization using high-contrast materials. The impact of such loading was investigated using both numerical simulations and measurements of the prototypes. The study finally led to a complete understanding of the miniaturization limitations associated with simple dielectric profiles. Insights were obtained from these initial investigations and such insights will provide important directions towards improving the amount of miniaturization.

Chapter 3

Baseline Design – Archimedean Slot Spiral Antenna

There are four main issues that are associated with the design of a spiral antenna. The first issue is making the antenna an efficient radiator by proper design of the spiral geometry. The other issues relate to the cavity backing for unidirectional radiation, the balun for broadband impedance matching and the arm termination to reduce reflections from the end of the spiral arm. The major challenge associated with the later issues is making them as broadband as the spiral antenna itself. The following two sections will discuss these issues and the methods used in the state-of-the-art design to address them. In the last section we then discuss improvements to the design and modifications that were necessary for the material loading of the spiral antenna.

3.1 General Spiral Antenna Design Issues

The operation of the spiral antenna is usually presented in terms of "radiation band" theory which states that the spiral predominately radiates from annular bands whose circumference is an integer multiple of a wavelength. Radiation occurs from these regions because the currents flowing in adjacent arms naturally become in phase leading to coherent/constructive radiation from the adjacent currents on the arms. Outside these regions the currents are not in phase and therefore the radiated fields tend to completely cancel each other. Typically, the two arm spiral is excited so that each arm has a current that is 180 degrees out of phase with respect to the other. For such an excitation the spiral can only radiate from regions where the circumference is an odd integer multiple of a wavelength. Specifically, radiation from the 1λ-circumference region will produce an omni-directional radiation pattern with the maximum at boresight. However, because the spiral is a traveling wave antenna it is not a 100%

efficient radiator which means that not all of the energy that enters the 1λ-circumference region will be radiated. Some energy is still confined to the antenna and continues to travel outwards where it can radiate from higher order regions (3λ, 5λ, etc.) if they exist or it can reflect from the end of the spiral arm. Radiation from higher order regions is undesired since it produces a null in the radiated pattern at boresight and a maximum at approximately 37 degrees from boresight. Therefore, any radiation from higher order regions will add to the radiation from the 1λ region which will lead to frequency dependent pattern distortion. Additionally, if the traveling wave is allowed to be reflected from the end of the spiral arm it will reverse direction and begin to travel inwards towards the center of the spiral. As it travels inward it will pass through the 1λ-circumference region for a second time but is traveling inwards instead of outwards. Therefore, the resulting radiation is cross-polarized to the first which will result in a total radiated field that is elliptically polarized. To prevent radiation from higher order regions and re-radiation from the 1λ region the spiral must radiate as much energy as possible in the 1λ-circumference region and any energy left over must be absorbed by the arm termination. For an Archimedean spiral this means that the growth rate and arm (conductor) width must be properly chosen and if necessary varied to maintain sufficient attenuation of the traveling wave through the 1λ region. This approach is sufficient to prevent radiation from higher order regions. However, at low frequencies where the 1λ region is located near or overlaps with the end of the antenna it is not enough. Thus, a broadband termination is needed to deal with the energy reaching the end of the spiral arm.

Since the Archimedean spiral is a quasi-frequency independent antenna [1] its bandwidth is theoretically only limited by is maximum size and the detail of the feed region. Therefore, the bandwidth of the antenna is typically limited by the method used to feed the antenna and the method used to make the spiral a unidirectional radiator. Therefore, the challenge is to make the feeding method and the spiral backing as broadband as the spiral itself.

The challenge with designing the feed (balun) is that it must concurrently have constant impedance over the entire band while also being well balanced to prevent squinted patterns and radiation from the feed structure which could disturb the input impedance and radiation pattern. Also, if the balun is to be integrated onto the spiral aperture it must not disturb the antenna fields. There are many baluns could be used to feed the antenna such as the infinite coaxial balun, integrated microstrip line, Marchand balun, impedance transformers, etc.. In choosing a balun

18

the most important characteristics are its bandwidth, loss and physical profile. Essentially, it is desired that the balun be very broadband, low loss and have a low profile.

The spiral antenna radiates a symmetric pattern equally well to the front and to the back. For most applications this is undesired since the antenna will be sensitive to anything placed behind it. Therefore, the antenna is made to radiate in one direction through the use of a ground plane or cavity backing. The use of a cavity allows the spiral to be mounted on or in structures so that unidirectional radiation is achieved. The use of a cavity is preferred since a finite size ground plane can be excited by the spiral and thus radiate to the backside much like a patch antenna. Additionally, if the spiral is to be conformally mounted the use of a cavity is unavoidable. The issue with any backing is to make it as thin as possible without negatively impacting the performance of the spiral. If the depth of the cavity is too shallow ($<\lambda/15$), a reduction of gain will occur due to excitation of a parallel plate transmission line mode. Excitation of this mode causes most of the energy to be coupled to this mode and guided to the end of the spiral arm where it will be dissipated in the termination thus reducing the gain. Therefore, a sufficient cavity depth is required at low frequencies to prevent this gain reduction. However, this depth usually becomes large at high frequencies leading to undesired cavity resonant modes which can be excited and cause the gain to drop near resonant frequencies, thus limiting the bandwidth of the spiral. The larger the cavity is made the smaller the bandwidth will be because the cavity mode resonances will occur at a lower frequency. Therefore, there is a trade-off between how deep the cavity should be to improve the low band response and how shallow it should be to limit the affects of cavity modes at high frequencies. Since the performance at low frequencies is very important, it is desired to make the cavity as deep as possible and to treat the cavity using techniques that will limit the cavity mode effects.

3.2 State-of-the-Art Baseline Design

In this section the methods used to address the issues presented in the previous section will be discussed for the state-of-the-art design shown in Figure 2.1. As it can be seen from Figure 2.1 the state-of-the-art Archimedean spiral design has multiple growth rates instead of one small growth rate which is typically associated with Archimedean spirals. The purpose of the multiple growth rates is to provide sufficient attenuation of the current through the 1λ region for a wide range of frequencies [1]. In [2] it was found that for Archimedean spirals a smaller

growth rate improved high frequency performance whereas a larger growth rate improved the low frequency performance. Therefore, the growth rate should be varied across the aperture to achieve optimal performance.

To deal with any energy reaching the end of the spiral arm a broadband Klopfenstein resistive taper was employed. This termination greatly reduces the cross-polarization and the axial ratio of the antenna by slowly attenuating the current as it reaches the end of the spiral arm [3]. This is achieved by using shunt resistive elements placed across a given length of the slot. Since the spiral cannot radiate efficiently from the region which is terminated, the length of the taper needs to be minimized. For this reason, the Klopfenstein taper is used since it provides the minimum taper length necessary to achieve a given reflection coefficient. This termination method is shown in Figure 3.1 where it is circled in red.

Klopfenstein
Resistive Taper

Infinite Coaxial
Balun
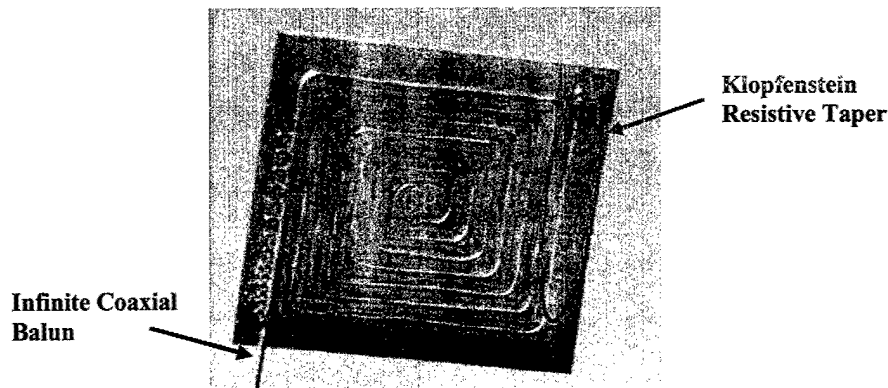
Figure 3.1 Square spiral illustrating the resistive termination and infinite coaxial balun used in the state-of-the-art design.

The current design uses an infinite coaxial balun because of its broad bandwidth and ease of implementation. Additionally, it can be mounted to the surface of the antenna without affecting the antenna fields (i.e. it has a very low profile). The infinite coaxial balun consists of a piece of coaxial cable that is soldered to the surface of the spiral along one of the spiral arms as shown in Figure 3.1. The balun then feeds the spiral at its center by exciting the two arms of the spiral equally and 180 degrees out of phase. This is done by stripping away the outer conductor in the feed region and extending the center conductor across the slot where it is soldered to the other arm. A shorted dummy cable is usually soldered to the other arm to provide both physical and electrical symmetry.

To address the cavity issue the cavity is made as deep as possible and a thin layer of absorber is used to line the walls of the cavity in order to eliminate cavity modes. Typically

many layers of absorber are used to attenuate the cavity. This leads to an attenuation of the field radiated from the backside of the spiral which also reduces the efficiency of the antenna. Furthermore, additional efficiency reduction is possible by the interaction of the antennas reactive near fields with the absorber if it is placed to close to the antenna. By using only a thin layer or layers of absorber the current cavity treatment effectively eliminates the cavity modes and minimizes reduction in the efficiency.

3.2.1 Square Slot-line Spiral Antenna Performance Verification

The gain of a previously constructed 6"x6" square slot-line spiral antenna prototype (see Figure 3.2) was measured at the OSU/ESL Compact Range facility for baseline performance verification. The resultant gain is very much the same to previously reported data. We remark the special meandered spiral arm design was used to lower the operational frequency.
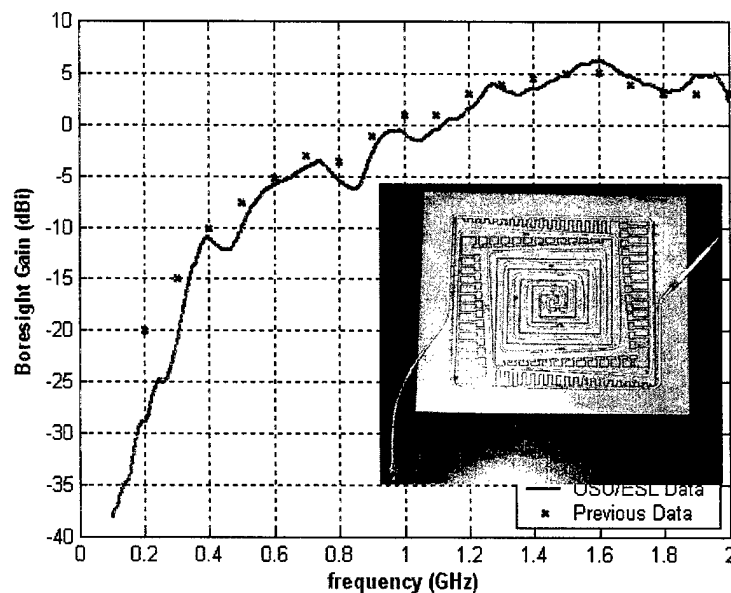
Figure 3.2 Comparison of gain measured at OSU Compact Range and previous data.

A numerical model based on the finite element method (FEM) code developed previously [4-7] was created for a 2"x2" slot-line spiral antenna design as shown in the insert of Figure 3.3. As seen, the calculated gain compares well with that obtained from the OSU/ESL Compact Range with an excellent agreement. This data verifies the accuracy of the numerical code and measurement results.
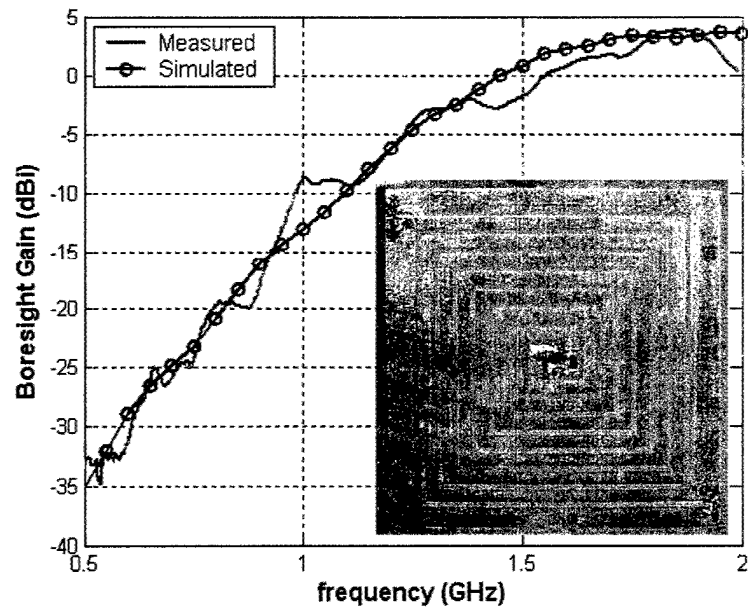
Figure 3.3 Measured and calculated gain for a cavity-backed 2"x2" slot-line spiral

3.2.2 Square versus Circular Spiral

The current state-of-the-art of small spiral designs using reactive loading is depicted in Figure 3.4. Table 3.1 summarizes their gain performance by providing the frequency at which the antenna first achieves a specified level of gain. Notice that a variable growth rate and meandering was used to improve the performance at low frequencies for these antennas. Nonetheless, the square version of the circular spiral performs better at low frequencies.
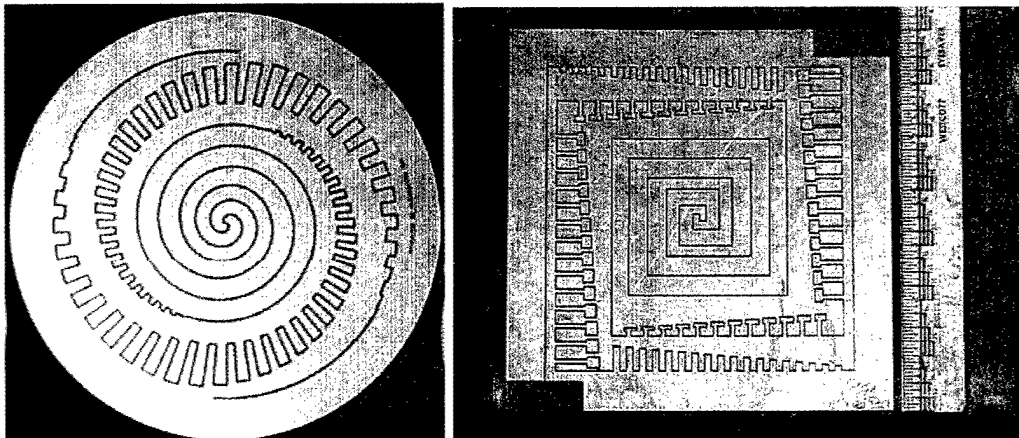
Figure 3.4 A Cavity Backed 6" Circular Slot Spiral with Meandering and the Equivalent Square Version

Gain (dBi)	-15	-10	-5	0
$f_{CIRCULAR}$ (GHz)	0.438	0.600	0.750	1.015
f_{SQUARE} (GHZ)	0.339	0.500	0.643	1.122

Table 3.1 Measured boresight gain for a 6" circular slot spiral with meandering treatment and a 6" square version shown in Figure 3.4.

3.3 Design Improvements

The purpose of this sub section is to discuss the modifications made to the balun and arm termination to facilitate the loading of the antenna and a lossless cavity mode suppression technique that was developed.

3.3.1 Balun

In preparation for the dielectric loading, a new feeding scheme was needed because the previous balun (shown in Figure 3.1) occupied the surface of the spiral which must be left bare for superstrate loading. To free the antenna surface from this spiraling cable, a 0°-180° broadband hybrid was employed instead. This hybrid uses a standard coax at the input, and its output is in the form of two coaxial cables with their outer conductors soldered together as shown in Figure 3.5. The hybrid serves to make the center conductors of the output cables opposite in polarity whereas the outer conductor provides the means for shielding, thus suppressing secondary radiation. Using this hybrid, the antenna can be fed from the substrate side through the use of two vias located on opposite sides of the slot at the center of the spiral (feed point). Therefore, the surface of the spiral is made free from the feeding structure allowing for loading of the spiral using a superstrate. In addition, during our investigation, it was found that the feeding cable arrangement adopted previously (see Figure 3.1) caused unstable gain values at very low frequencies. We suspected that this was caused by cable radiation and scattering. This problem has been overcome with the new balanced feeding arrangement via a 0°-180° Hybrid located at the spiral center. This is demonstrated by comparing the measured gains of the 2"x2" spiral antennas using these two different feeding arrangements as shown in Figure 3.6. The abnormal gain variations at low frequencies have been greatly reduced. The higher axial ratio (resulting from the cable scattering/radiation) is also significantly improved as demonstrated in Figure 3.7.

23

Another distinct advantage of the hybrid balun in that it does not suffer from cable loss. This is because the hybrid balun only requires a section of cable that is slightly longer than the depth of the cavity which is only a couple of inches. On the other hand, the length of the cable required for the coaxial balun it typically on the order of a couple feet and will therefore have significantly more cable loss.
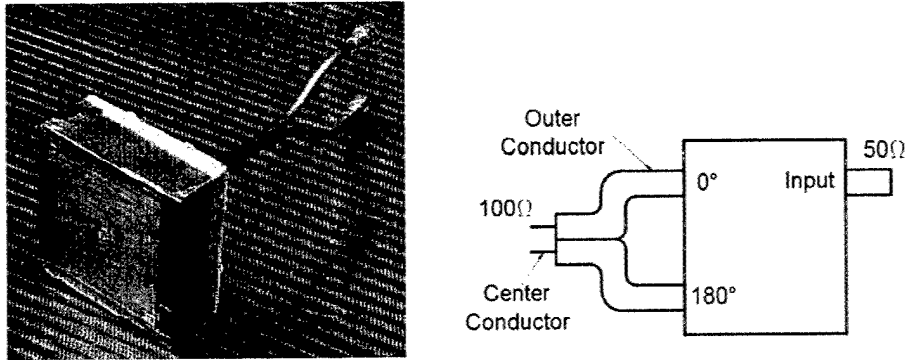
Figure 3.5 New 0°-180° Hybrid Balun.
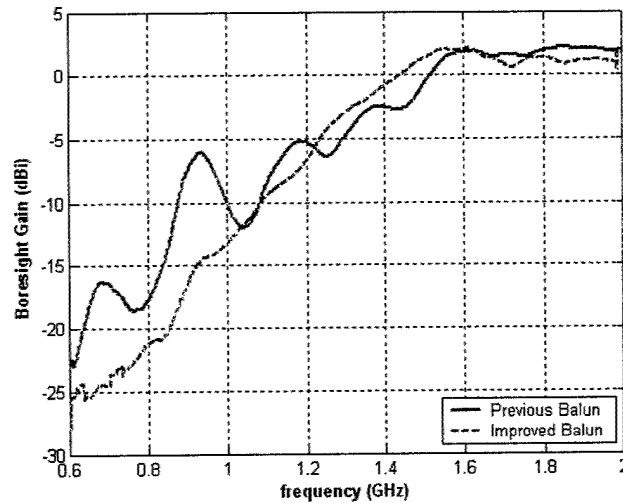
Figure 3.6 Measured Gain of the 2"x2" spiral antennas fed with the previous infinite balun and with the new 0°-180° hybrid balun.
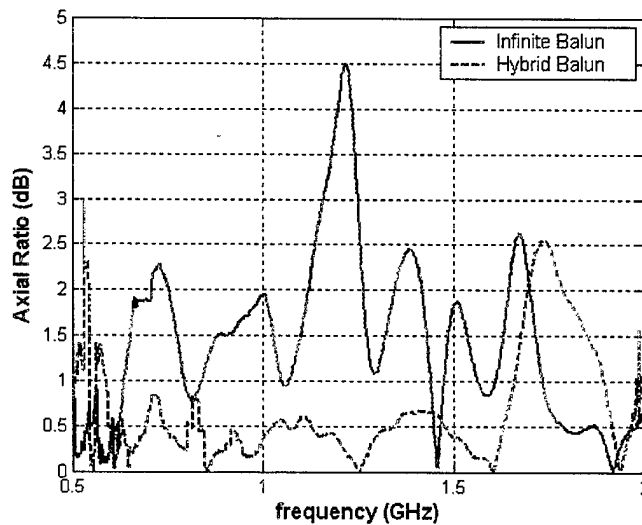
Figure 3.7 Measured Gain of the 2"x2" spiral antennas fed with the previous infinite balun and with the new 0°-180° hybrid balun.

3.3.2 Arm Termination

The previously employed termination was based on a Klopfenstein resistive taper which used multiple chip resistors placed along a properly chosen length of the arm (see Figure 3.8). As mentioned previously, this served to slowly attenuate the current before it reached the end of the spiral arm. It has been shown to be very effective in minimizing reflections from the end of the spiral arm without a priori knowledge of the slot impedance. However, this termination occupies a significant length of the spiral arm which limits a portion of the aperture's utility and the dielectric loading of that same portion. Leaving any portion of the antenna unloaded that is associated with radiation from low frequency components is not desired since it would reduce the amount of miniaturization. An improved (not optimal) alternative would be to use a single termination resistor located at the end of the slot line. This new arrangement is shown in Figure 3.8 and it allows for greater utilization of the spiral aperture. Additionally, as shown in Figure 3.9, it provides better axial ratio (polarization purity) at low frequencies compared to the previous termination method. This can also be seen from Figure 3.10 which shows the decomposition of the gain into its left hand circular polarization component G_L and the right hand circular polarization component G_R for the two termination cases. For the winding sense of this spiral the G_L component is the desired polarization and the G_R component is the component

25

which contributes to cross-polarization. It is evident that the single resistor termination improves the cross-polarization at low frequencies and there by improves the axial ratio.
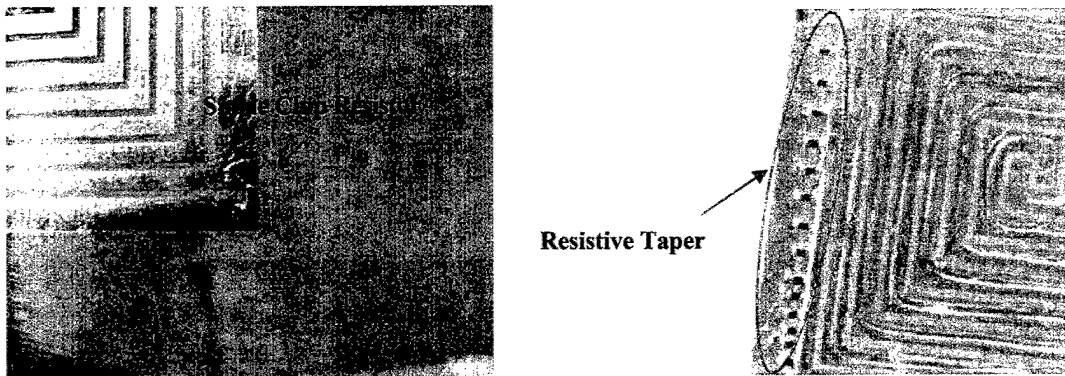
Figure 3.8 Single-resistor vs. multiple-resistor termination of spiral arms.
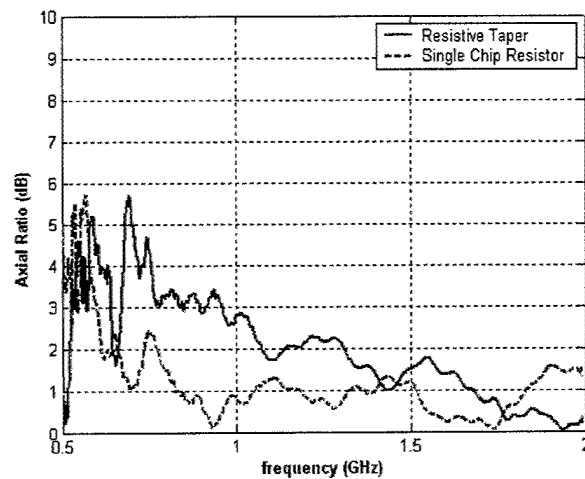
Figure 3.9 Measured axial ratio comparison of single-resistor termination vs. tapered resistor termination.
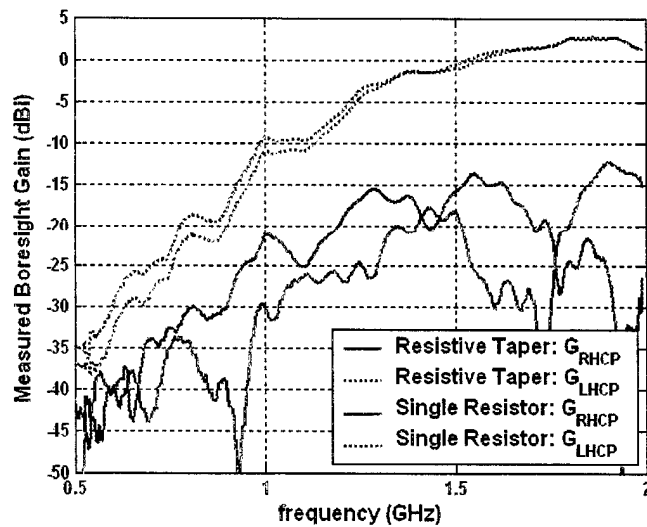
Figure 3.10 Gain decomposition into LHCP and RHCP components.

3.3.3 Cavity Mode Suppression

Several techniques for suppressing cavity resonances were investigated previously [2]. One of them is to add absorber lining inside the cavity to damp the resonance. This approach was shown to be quite effective for suppressing the undesired cavity modes. However, it also reduces antenna efficiency (and therefore gain) in the process. A new cavity mode suppression method was investigated without the lossy wall absorber. Our approach introduces a layer of radial wires into the cavity at an optimal distance from the antenna aperture as shown in the inset of Figure 3.11. Away from the center, the spacing of the radial wires is large enough to have no impact on the low frequency operation which effectively makes the cavity deeper. Near the center, the depth of the cavity is reduced to where the radial wire is located. The improvements obtained by using this new approach can be clearly seen in Figure 3.11 (red curves). From this figure it is evident that this new technique works by shifting the cavity modes to higher frequencies instead of attenuating them. Thus gain reduction does not occur at high frequencies as seen with the absorber treatment. This is readily observed from the region in Figure 3.11 which is highlighted by the dashed red circle.

27
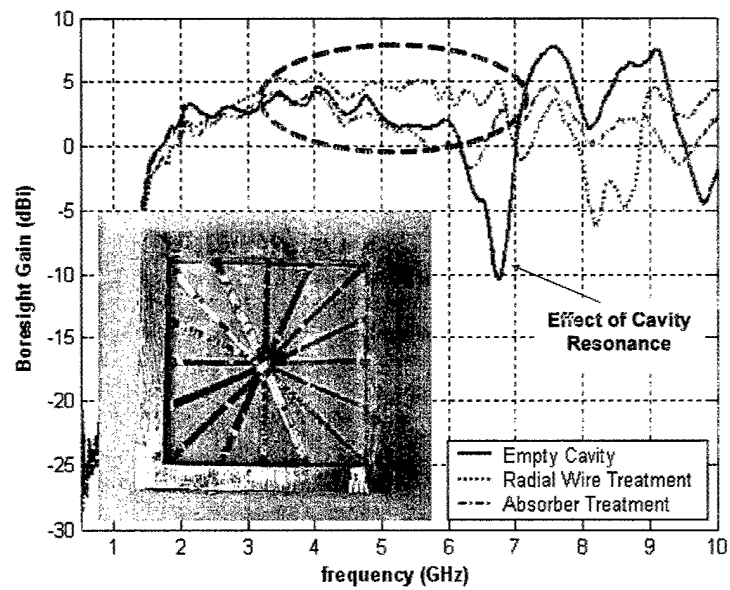
Figure 3.11 Measured gain of a 2"x2" spiral with and without cavity treatment.

Chapter 4

Antenna Miniaturization using Dielectrics

The purpose of this chapter is to provide an understanding of how the spiral antenna can be miniaturized using materials and the limitations of miniaturizing the spiral antenna using simple material profiles or topologies. The first section will discuss the concept of miniaturizing the spiral antenna and the following section will briefly discuss the criteria used to measure the miniaturization of a broadband antenna. The remaining sections will discuss the miniaturization, issues and limitations of using dielectric materials.

4.1 Concept

The concept of miniaturizing the spiral antenna is readily explained by the radiation mechanism of the spiral antenna. The spiral antenna radiates because currents flowing in adjacent arms naturally become in phase in regions (active region) where the circumference is an integer multiple of one wavelength. In this region, the coherent phase condition that exists between the currents in adjacent arms leads to strong constructive radiation. For a circular spiral this occurs at a diameter D that is an integer multiple of λ/π and for the square spiral when the diameter is around $\lambda/4$. Therefore, the active region for high frequencies is located near the center of the spiral and as the frequency is reduced the active region moves outwards from the center. Since the location of the active region is frequency dependent it is therefore dependent upon the wavelength in the antenna structure. Thus, material loading of the antenna can control the location of this active region for a given frequency as illustrated by the following equation

$$D = \frac{\lambda_g}{4} = \frac{\lambda_0}{4\sqrt{\mu_e \varepsilon_e}} \qquad (1.1)$$

where μ_e and ε_e are the effective relative permeability and permittivity. From equation (1.1) it is apparent that material loading results in a reduction of the active region diameter by shifting the active regions towards the center of the spiral. The amount of shifting depends upon the effective dielectric constant obtained by loading the antenna. If the antenna were loaded by an infinite half-space or full-space the effective dielectric constant is as follows

$$\varepsilon_e = \begin{cases} \sqrt{(\varepsilon_r + 1)/2} & \text{, for infinite half - space} \\ \sqrt{\varepsilon_r} & \text{, for infinite full - space} \end{cases} \tag{1.2}$$

However, for finite loading, only a fraction of one of these cases is obtainable and the amount is dependent upon the configuration of the loading such as the thickness, width, shape and so forth. Specifically, the combination of the loading geometry and the antenna near field distribution determine the effective dielectric constant.

4.2 Miniaturization Criteria for Broadband Antennas

One challenge associated with miniaturizing any broadband antenna is defining the criteria used to measure the amount of miniaturization. The reason for this can be clearly illustrated by considering a narrowband antenna. For narrowband antennas determining the amount of miniaturization is very straightforward if the resonant frequency is used as the reference point. This is because the resonant frequency can be easily defined in terms return loss, gain or input impedance and, as a result, it is easily distinguishable. Therefore, the effects of material loading are easily observed by comparing the location of the resonant frequency for the loaded and unloaded cases.

For broadband antennas the choice of a reference point is not as obvious as illustrated in Figure 4.1. This is because broadband antennas lack a distinguishable frequency that can be consistently characterized in terms of various antenna parameters. For the spiral antenna, one would ideally like to use as the reference point the lowest frequency at which the first active region can be supported by the spiral diameter. However, the parameters such as gain, return loss and impedance that can be used to characterize this point are very sensitive to changes in the spiral's geometry even if the diameter of the spiral is held constant. Therefore, using this point to measure the loading affect is not an optimal choice. What is needed is a reference point that depends on as few factors as possible. One such point is the frequency at which the spiral

antenna first achieves a gain of -15dBi. The only factors that influence its location besides material loading are the physical size of the spiral, radiation efficiency (arm termination), and mismatch losses. As long as the arm termination remains the same for all cases and mismatch losses are minimized by proper matching then the only factors that influence this point are the loading affects and physical size just as desired. Therefore, the -15dBi gain point will be used as the reference point from here on.
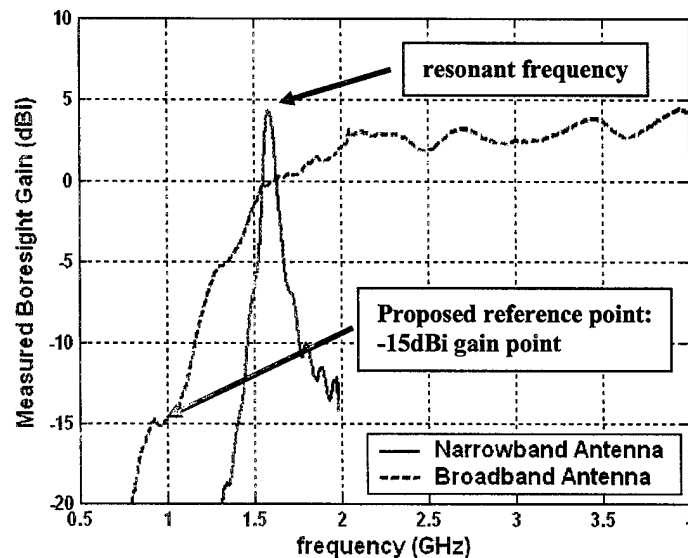
Figure 4.1 Illustration of the difference between the miniaturization criteria used for narrowband and broadband antennas.

4.3 Dielectric Loading Configuration

In this section the affects of loading the square spiral with a uniform square dielectric slab will be characterized. First, only a single side is loaded and the impact of the slab thickness and width are studied. Then, the effect of loading both sides of the antenna is examined. This is followed by some initial experimental results obtained from loading the spiral (2" and 6" square spirals).

4.3.1 Single-Sided Loading

The following figure shows a cross section of the loading geometry that will be considered in this sub section. It consists of a 53mm diameter square spiral in free space which is

loaded with a square slab of dielectric material of thickness t, width L and uniform dielectric constant ε_r.
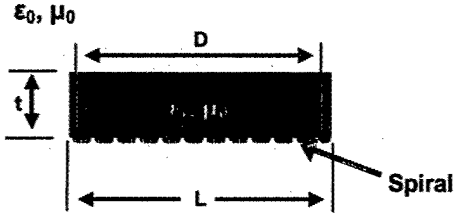
Figure 4.2 Finite Single-Sided Loading Geometry.

To study the impact of the slab thickness on the shifting of the -15dBi gain point the width of the slab is held constant by setting it equal to the diameter of the spiral. The thickness of the slab was then varied for two cases where the dielectric constant was 9 and 16 respectively. The miniaturization factor (MF) associated with the -15dBi gain point was then calculated by using the following equation:

$$MF = \frac{f_{unloaded,-15dBi}}{f_{loaded,-15dBi}}$$

(1.3)

The results are shown in Figure 4.3 where the horizontal dashed lines represent the MF achievable for a dielectric constant of 9 (blue) and 16 (green) if the antenna was loaded with an infinite half-space. As it can be seen in Figure 4.3, there is an initial rapid increase in the MF for both cases but convergence is quickly achieved as the thickness is increased further and stops well short of the maximum achievable miniaturization. It is apparent from this figure that once the thickness is thick enough a further increase in thickness, no matter how large, will result in little further miniaturization.
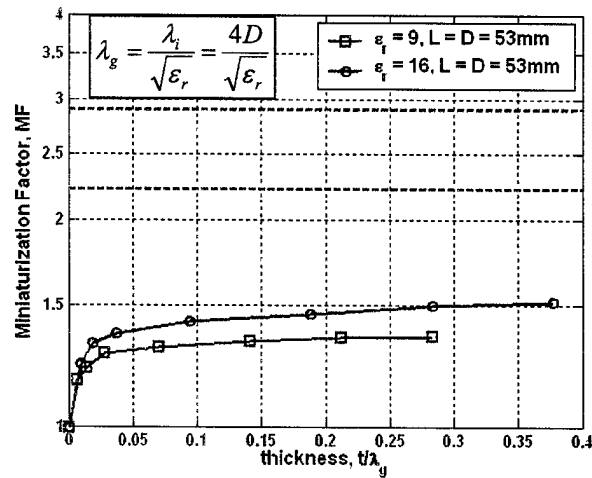
Figure 4.3 MF as a function of the material loading thickness in guided wavelengths λ_g.

The reason for this is that the low frequency fields of the spiral antenna extend outside the aperture of the antenna as depicted in Figure 4.4. Therefore, no matter how thick the superstrate is, the fields in this region (circled in yellow) never see the dielectric material and thus limit the amount of miniaturization. The only way to increase the miniaturization for a given dielectric constant is to load these fields by increasing the width of the slab.
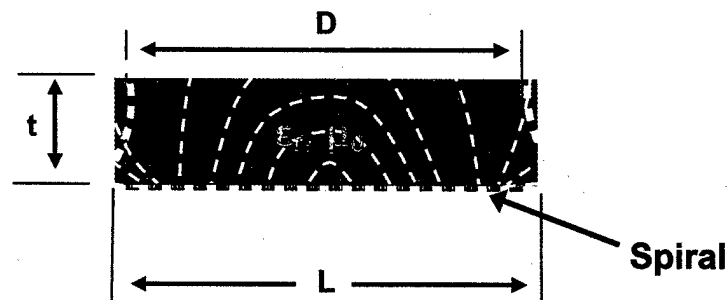
Figure 4.4 Illustration of Electric field lines of the spiral antenna.

Figure 4.5 shows the results obtained by increasing the width of the slab for a thickness of $0.212\lambda_g$. From this figure it is evident that the miniaturization is increased further as the width is increased thereby confirming the assumption that the low frequency fields extend outside the

33

aperture of the antenna. Therefore, it can be inferred that the maximum MF for any dielectric constant is achievable as long as the fields of the antenna are loaded sufficiently. However, sufficient loading of the antenna fields in this manner is not practical since it increases the overall diameter of the antenna. Consequently, it can be concluded that the achievable MF for a specified dielectric constant is constrained by the width of the antenna and is limited by the thickness which can be tolerated.

The practical limitations on MF for a given thickness and dielectric constant will be discussed in section 4.5. It should be noted that having the antenna diameter to be the same as the slab width is always advantageous unless an extremely high dielectric constant is used (>240) which is not preferred at this time due to reasons that will be discussed in more detail in section 3.4.
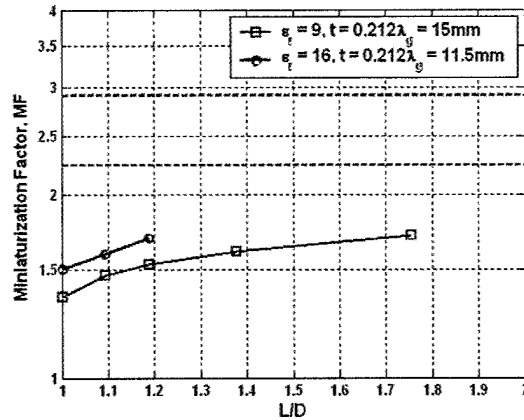
Figure 4.5 Impact of superstrate width on MF.

4.3.2 Double-Sided Loading

In the previous section the results for loading only a single side were presented. However, for a given thickness t, is it more advantageous to load only one side with a slab of thickness t or to load both sides each with a slab of thickness 0.5t. To answer this question both sides of the spiral antenna were loaded with a square slab. The results were then compared to those obtained from the loading of only a single side by considering the total thickness of the material used to load the antenna as illustrated in the following figure.

Cross Section

Single-Sided Loading

Square
Spiral

Double-Sided Loading
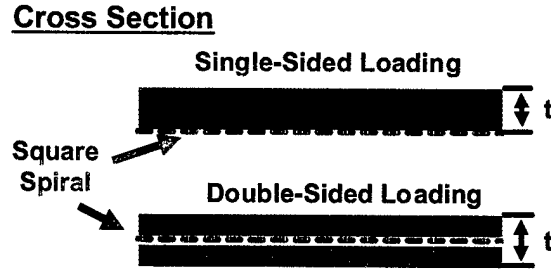
Figure 4.6 Cross section of single-sided and double-sided loading.

Figure 4.7 shows the comparison between loading only a single side (blue) and loading both sides using a dielectric constant of 9. It is observed that for the same total thickness more miniaturization is achieved when both sides of the antenna are loaded. This observation is true as long as the total thickness is greater than 0.025λg. Therefore, it can be concluded that loading both sides of the antenna maximizes the amount of miniaturization if the material is sufficiently thick. This is due to the fact that for a given total thickness one can effectively load more of the antenna fields by loading both sides of the antenna.
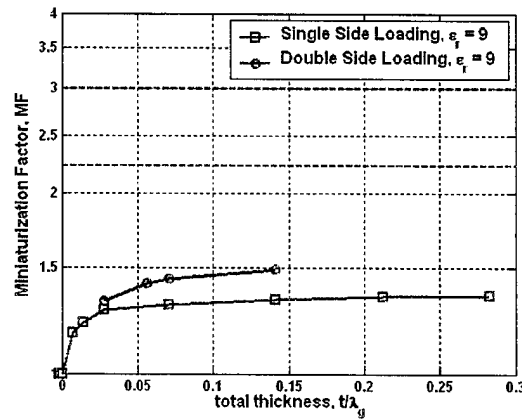
Figure 4.7 Comparison of the MF for single-sided and double-sided loading.

4.3.3 Initial Experimental Results for Dielectric Loading

To experimentally demonstrate the concept of miniaturization using high-contrast material loading, a 2" square spiral antenna prototype was initially used due to its convenient frequency range and size. High dielectric layers with thicknesses of 2mm or 3mm and dielectric constants of 37 and 90 were individually placed on top of the spiral antenna as illustrated in Figure 4.8. The gain of the dielectric loaded antenna was measured and compared with that obtained from the no-loading case as shown in Figure 4.8. It is important to mention that no

resistive termination was used in this trial and the antenna is not well matched. Thus, we observe variations in the gain curve due to the reflections from the end of the spiral arm.

Table 4.1 summarizes the findings of the frequency shift at the −15 dB gain point. Note that the -15dBi gain point for the unloaded spiral is at 895 MHz. The introduction of a dielectric superstrate on the slot-line spiral clearly moves the gain curve toward lower frequencies. The amount of shifting is also greater for the higher dielectric constant (i.e. 90) and larger thickness (3mm). The largest MF of 1.5 is obtained from loading the antenna with a dielectric constant of 90 and thickness of $0.089\lambda_g$. Such a reduction can be predicted from the analysis and will be shown later.
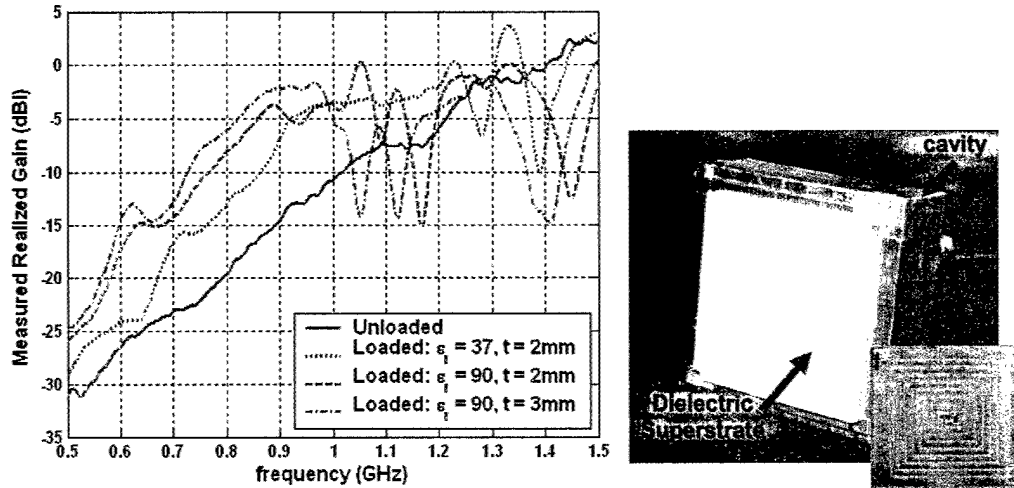
Figure 4.8 Measured gain of a 2" square spiral with and without a dielectric superstrate (measured with cavity without termination resistor).

ε_r	t/λg	f_L(-15 dBi)	MF=f_0/f_L	% Reduction
37	0.038	763 MHz	1.172	14.7
90	0.059	633 MHz	1.414	29.3
90	0.089	598 MHz	1.497	33.2

Table 4.1 2" square spiral summary for the frequency shift of the -15dBi gain point.

To verify that the miniaturization behavior observed in the 2"x2" prototype could be obtained for larger apertures a 6"x6" square spiral antenna prototype was also fabricated and tested for gain with and without the high-dielectric superstrate loading. The 6" spiral prototype is the same design as the 2" prototype with additional turns to make it 6" in diameter.

Figure 4.9 shows a comparison of the measured gain values for the unloaded case (blue curve) and the loaded case (green curve) with uniformly thick superstrate of $\varepsilon_r = 30$. The loaded case has lower gain at higher frequencies (>0.5 GHz) due to additional impedance mismatch loss created by the material loading. However, note that the same reduction of the -15 dBi gain point was still achieved. In addition, it was found that the gain obtained from the 6"x6" dielectric loaded prototype agreed well (particularly in the roll-off region) with that observed in the 2"x2" prototype of a similar dielectric loading. This is shown in Figure 4.10 where the dielectrically loaded 6" prototype is being compared to the loaded 2" spiral by scaling the 2" spiral results in frequency by a factor of 3.
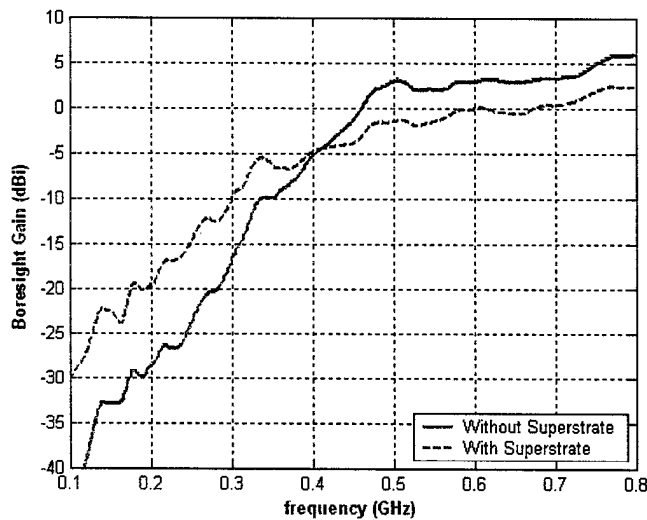
Figure 4.9 Measured gain of 6" square spiral with and without a dielectric superstrate (ε_r = 30).
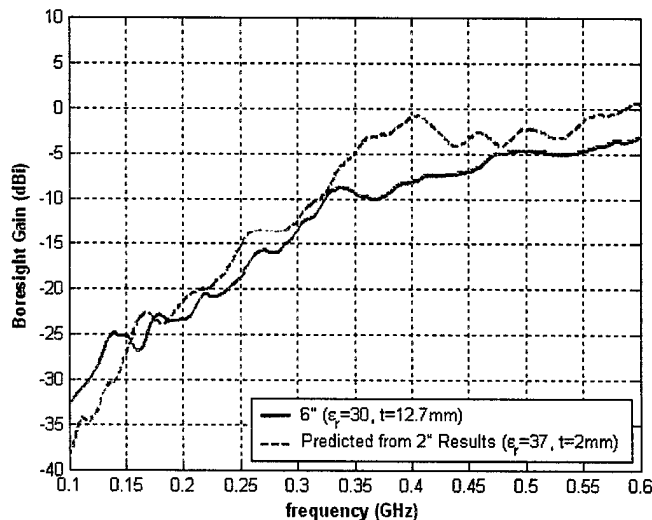
Figure 4.10 Comparison of gain measured from 6"x6" prototype with the frequency-scaled gain measured for a 2"x2" prototype.

4.4 Dielectric Loading Issues

As shown in Figure 4.9, dielectric loading not only shifts the gain curve to lower frequencies but it will also increase the mismatch losses at high frequencies which will reduce gain if not properly compensated. This section will discuss the issue of input resistance reduction that is associated with dielectric loading. In addition, solutions to address this problem will be discussed and demonstrated.

4.4.1 Input Resistance Reduction

Since the spiral radiates from different regions depending upon the frequency, uniform dielectric loading results in a non-uniform loading of the individual frequency components. Essentially, the electrical thickness of the superstrate is much larger for the higher frequencies than the lower frequencies. Therefore, the higher frequencies are being scaled more and, as a consequence, their impedance is reduced more than the low frequency components. This is undesired and unnecessary since it is the low frequency components that we wish to scale.

A consequence of dielectric loading there is a reduction in the input resistance of the antenna. As shown in Figure 4.11, increasing the thickness of the dielectric slab leads to further reduction in the input resistance. In fact, the input resistance asymptotically approaches a value which is equal to the unloaded value divided by the square root of the effective dielectric constant. From this observation it can be inferred that loading both sides of the antenna will result in even more reduction due to the larger effective dielectric constant that is obtained by the loading of both sides. From Figure 4.12 it is evident that double-sided loading results in more reduction.

38
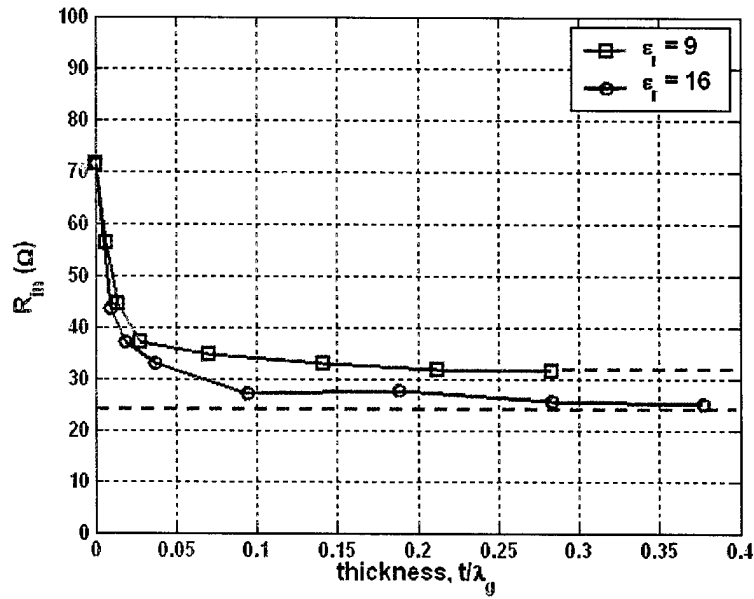
Figure 4.11 Impact of superstrate thickness on input resistance reduction for single-sided loading.
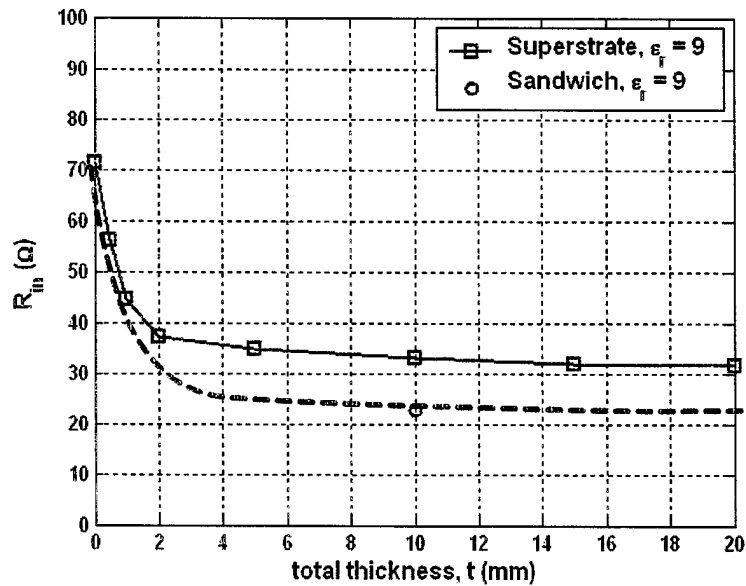
Figure 4.12 Comparison of input resistance reduction for single-sided and double-sided loading.

The reduction in the input resistance is a problem for several reasons. First of all, it will lead to an increase in mismatch losses unless the impedance of the balun is lowered to match the reduction or the geometry of the spiral is changed to increase its impedance in order to counter the reduction. For the spiral, it is not desired to alter the impedance significantly because this will

39

reduce the amount of attenuation of the traveling wave through the first active region which is undesired. Therefore, changing the impedance of the spiral can only provide so much compensation. Consequently, it the loading reduces the impedance significantly then the hybrid balun will have to be redesigned or the profile of the material could be altered to help alleviate the problem. The second reason why a drop in the input resistance is an issue is because of its relation to the radiation resistance of the antenna. While the input resistance is not equal to the radiation resistance, it is directly related to it. Therefore, a decrease in the input resistance will lead to a decrease in the radiation resistance which determines the amount of power radiated by the antenna. The larger it is, the more power the antenna can radiate. However, the radiation resistance does not affect the gain of the antenna since the gain is a measure of how efficiently an antenna can spatially focus energy. Therefore, a lower radiation resistance means that the antenna will deliver less power to a receiving antenna as long as the gain and the power delivered to the antenna remain unchanged. This may or may not be an issue if the power delivered to the antenna can be increased as desired.

Whether or not the drop in radiation resistance is a problem, the use of high contrast materials presents a challenge from an impedance matching point of view. However, this becomes less of a problem if the antenna is loaded in an intelligent way such that the impedance reduction is minimized. One possible approach is to use a tapered profile (thickness or dielectric constant) of the dielectric material. Other possible solutions to this problem are using magnetic material to increase the impedance and possibly the inclusion of lumped inductive loading to emulate the effects of magnetic material. All of these methods will be discussed in the following sub section starting with dielectric tapering.

4.4.2 Solution Methods for Input Resistance Reduction

4.4.2.1 Dielectric Tapering

The concept of dielectric tapering is to maintain the same electric thickness of the loading across the aperture of the spiral. That is the thickness or dielectric constant of the superstrate is varied such that the electrical thickness is the same across the aperture of the spiral. Thus, uniform loading is achieved and the reduction of the input resistance is minimized but not eliminated. An example of dielectric tapering is shown in the following figure. In this figure the

dielectric constant of the slab has been varied linearly starting with a dielectric constant of 3 at its center and ending with a dielectric constant of 9 in the outer region.
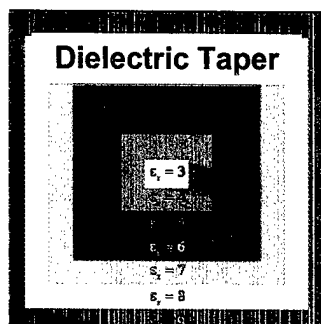
Figure 4.13 Top view of a dielectric slab which has a linear tapering of its dielectric constant.

A square spiral antenna was loaded using a uniform dielectric slab with $\varepsilon_r = 9$ and the dielectric slab shown in Figure 4.13. Figure 4.14 shows a comparison of the input resistance reduction for these two loading cases as a function of thickness. From this figure it is evident that the dielectric tapering treatment results in less reduction of the input resistance for the same thickness. However, this treatment is only useful if the same frequency reduction can be achieved as in the uniform case. As shown in Figure 4.15 the gain curves for the uniform slab and the dielectric tapered slab are almost identical. Therefore the same reduction in frequency is achieved if the tapering is implemented properly.
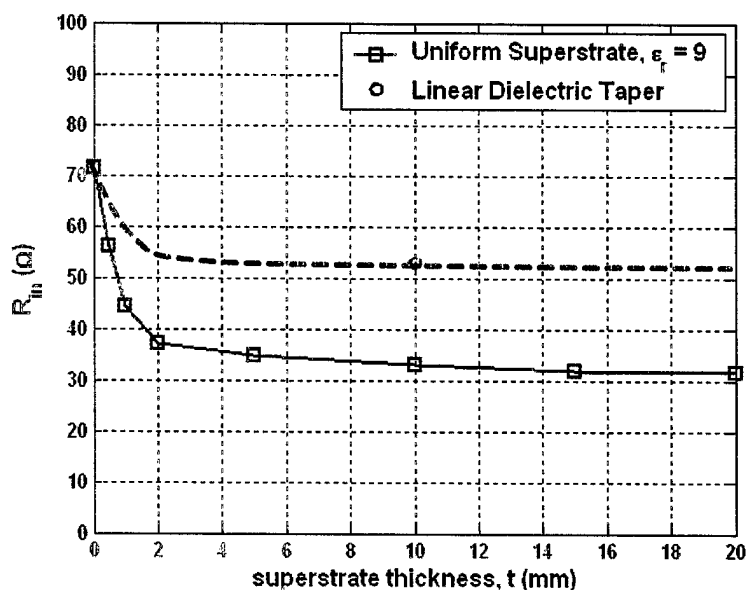
Figure 4.14 Effect of dielectric tapering on input impedance reduction.
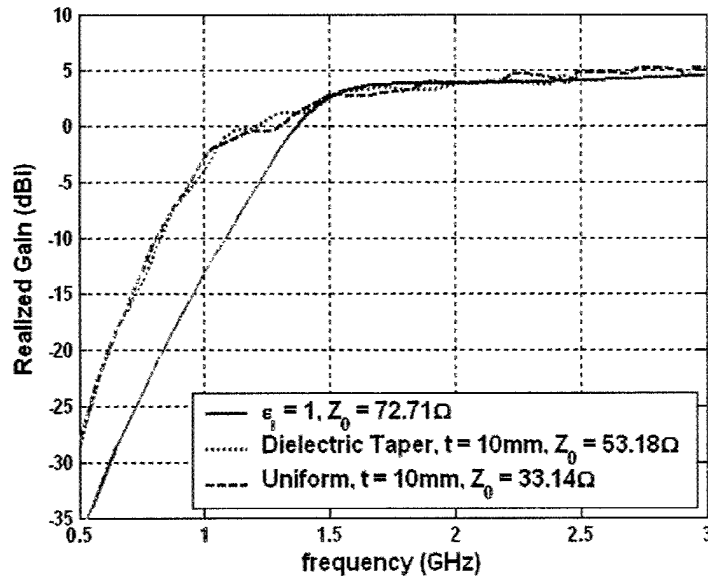
Figure 4.15 Effect of dielectric tapering on miniaturization.

4.4.2.2 Magnetic Material Loading for Impedance Improvements

Since dielectric tapering still results in a reduction of the input resistance it is desired to investigate methods that would maintain the input resistance. The use of magnetic material provides a means for maintaining the input impedance by essentially counter acting the effects of dielectric material. This is illustrated in Figure 4.16 where it can be seen that using the same μ_r and ε_r to load then antenna results in less reduction than dielectric tapering alone. However, there is still a reduction in the input resistance which implies that the fields of the spiral antenna interact differently with the magnetic and dielectric material. Basically, the magnetic material doesn't interact as strongly with the spiral antenna as does the dielectric material. Therefore, to maintain the input resistance it will probably be necessary to use a higher μ_r than ε_r. However, further investigation is needed to not only confirm this but understand how the two types of material interact with the spiral antenna.
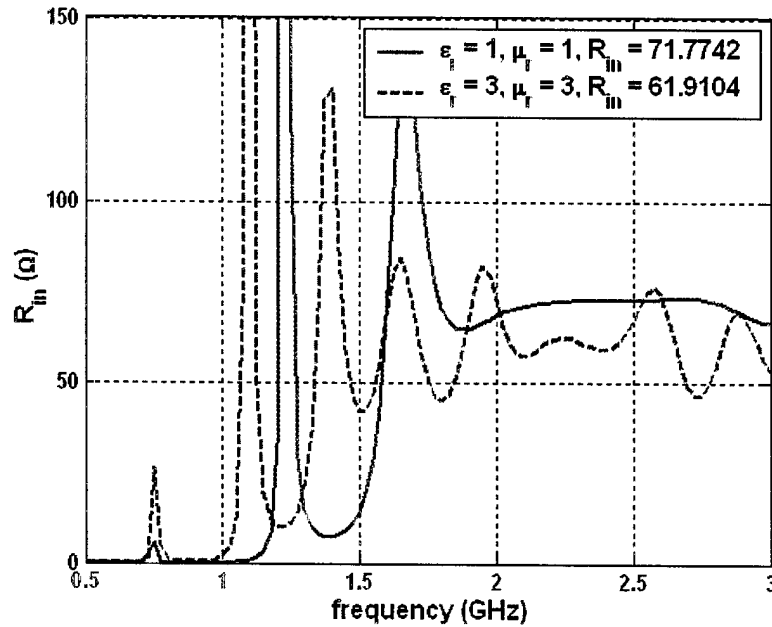
Figure 4.16 Influence of magnetic material loading on input impedance.

As mentioned previously, the problem with magnetic material is that it is currently narrowband and lossy particularly at high frequencies. Thus, its application is not practical unless the frequency is less than 100 MHz. Therefore, magnetic material has the potential to eliminate the input resistance reduction but it is not a practical option at this point in time. The best choice and most practical approach is dielectric tapering and an experimental example of its effectiveness will be shown in the following sub section.

4.4.3 Initial Experimental Results for Dielectric Tapering

As mentioned previously the loading of the 6" prototype suffered a decrease in gain at high frequencies due to increased mismatch losses. This is clearly illustrated in Figure 4.17 which shows the measured return loss of the 6" prototype for both the unloaded and the loaded case. From this figure it is apparent that the uniform dielectric slab causes a significant deterioration in the return loss.

43
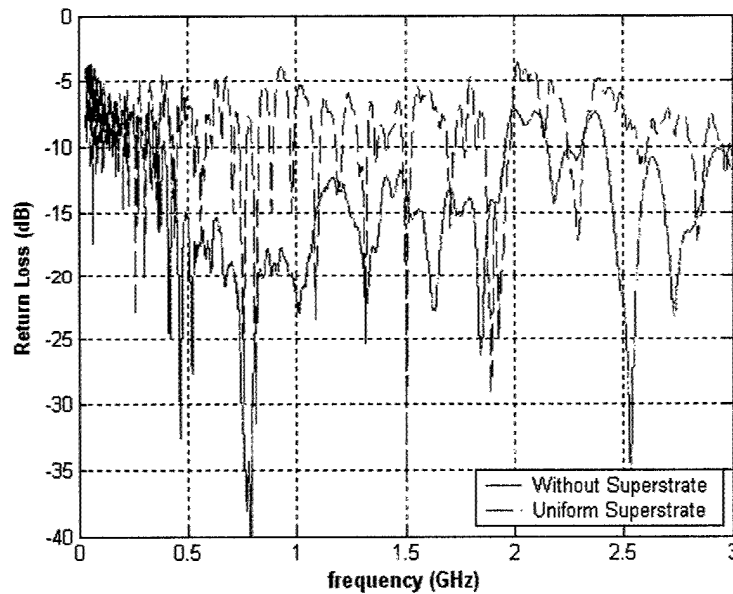
Figure 4.17 Measured return loss (dash-dot line) and without (solid line) a UNIFORM superstrate (ε_r=30).

To verify experimentally that the concept of dielectric tapering can be used to improve impedance matching, the uniform dielectric slab used to load the 6" spiral was altered by tapering the thickness of the slab. The slab was tapered by first cutting the square section into four triangular pieces using a diamond blade. Then, each smaller piece was further machined using a carbide milling bit into a section having a triangular cross section as shown in Figure 4.18. The four pieces were finally assembled and placed on the square slot spiral aperture using a low loss epoxy. As shown in Figure 4.19, the tapered superstrate significantly improves the return loss by limiting the amount of input impedance reduction as demonstrate by the previous simulations. Nonetheless, it has not eliminated it because the presence of the dielectric has still reduced the input resistance of the antenna. Therefore, to completely eliminate the mismatch loss the impedance of the balun or antenna must also be changed. Additionally, one can see from Figure 4.20 that the tapering does not effect the frequency reduction which is also in agreement with the simulated results presented earlier.
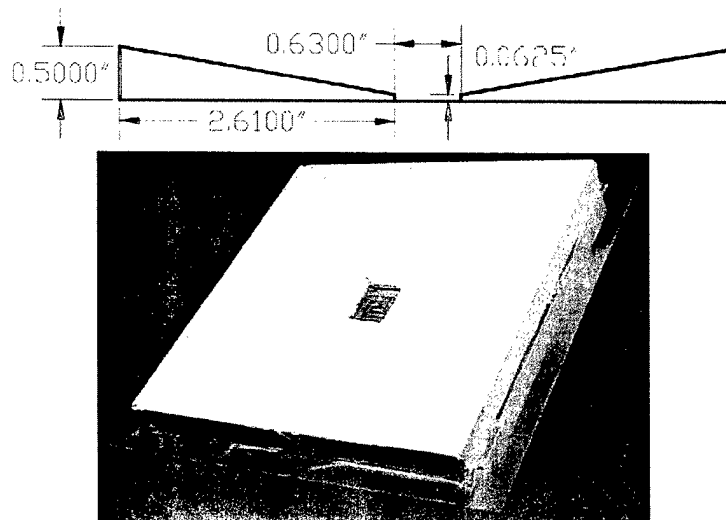
Figure 4.18 Cross section and picture of the thickness tapers dielectric superstrate for the 6" square Archimedean spiral.
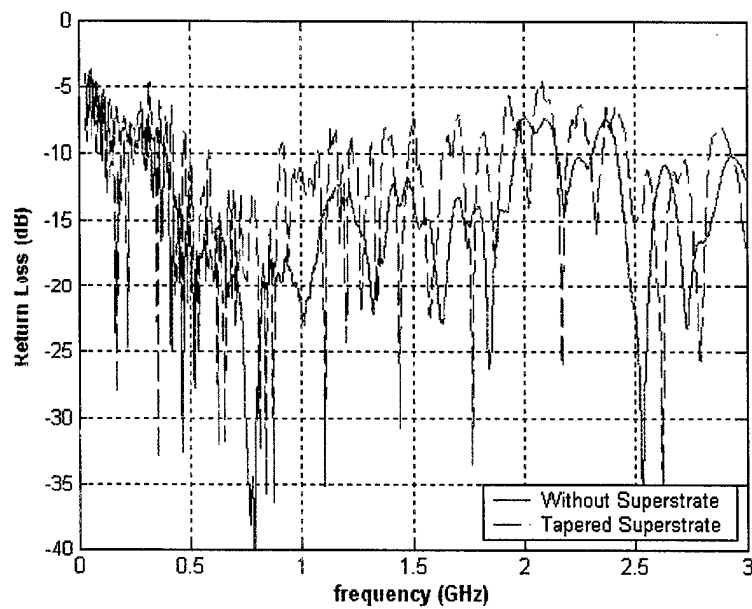
Figure 4.19 Measured return loss with (dash-dot line) and without (solid line) a TAPERED superstrate (ε_r =30).
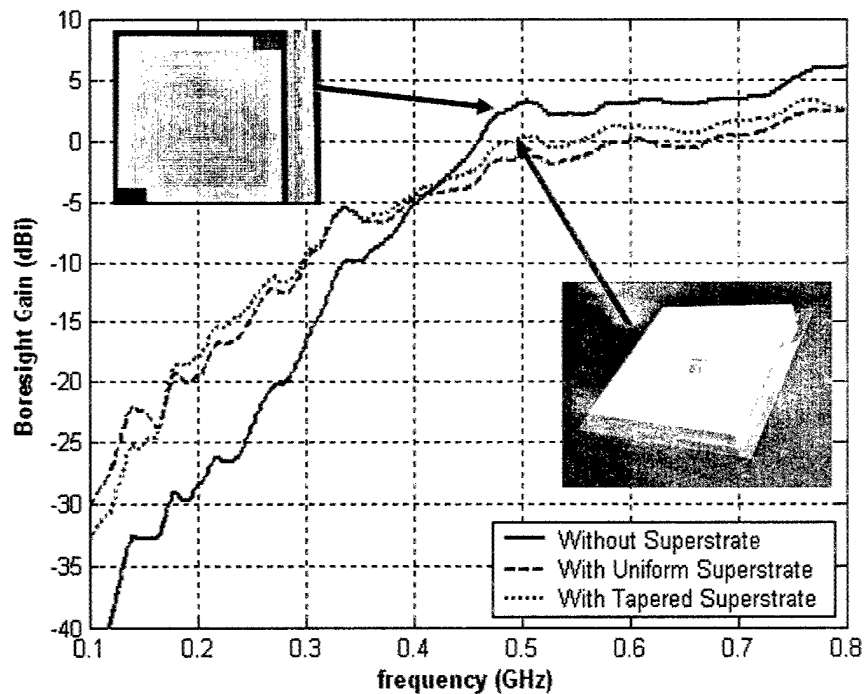
Figure 4.20 Measured gain of a 6"x6" square slot spiral antenna with and without high dielectric superstrate loading (ε_r=30, thickness=0.5 inches).

4.4.4 Miniaturization Limitations of Simple Dielectric Loading

In sub section 3.3.1 it was shown that by sufficiently loading the fields near the spiral antenna, one could approach the MF for the infinite half-space case. However, to obtain such a MF, the loading configuration had to be significantly larger than the antenna making it impractical. For a practical loading configuration where the width of the slab is equal to the diameter of the spiral it was shown that there was a limit to the amount of miniaturization one could achieve by increasing the thickness for a specific ε_r. Therefore, there is also a practical limit to the thickness of the slab. Considering that the antenna must be as low profile and as light weight as possible a thickness of $0.1\lambda_g$ is reasonable choice.

The question now becomes whether is there a limit to the amount of miniaturization that can be achieved by increasing ε_r? Figure 4.21 shows the behavior of the MF as a function of ε_r for two different cases (single-sided loading). The blue curve is for the infinite half-space case and therefore represents the limiting MF that can be achieved using a given ε_r. This curve was obtained from the theoretical relation between the MF and the effective dielectric constant which is as follows

$$MF = \sqrt{\varepsilon_e} = \sqrt{\frac{\varepsilon_r + 1}{2}} \qquad (0.1)$$

The other curve was obtained by using the results shown in Figure 4.3 to obtain the data points in Figure 4.21. These data points were then curve fitted to a function using the least squares (LS) approach. This was done by fitting the data points to the theoretical half-space curve weighted by some unknown coefficient. The LS method was then used to find the coefficient for the curve. As it can be seen from Figure 4.21, the weighted curve fits the data points very well.

It is evident from Figure 4.21 that for the $0.1\lambda_g$ thick dielectric slab a MF of 1.6 can be achieved using an $\varepsilon_r = 100$. In addition, it is apparent that a further increase in the dielectric constant will only result in small improvements while severely reducing the impedance. Therefore, there is always a tradeoff between size reduction and impedance reduction when only dielectric material is used to load an antenna. Furthermore, it can be concluded that for practical single sided loading profiles MF of 1.4 to 1.67 are achievable.
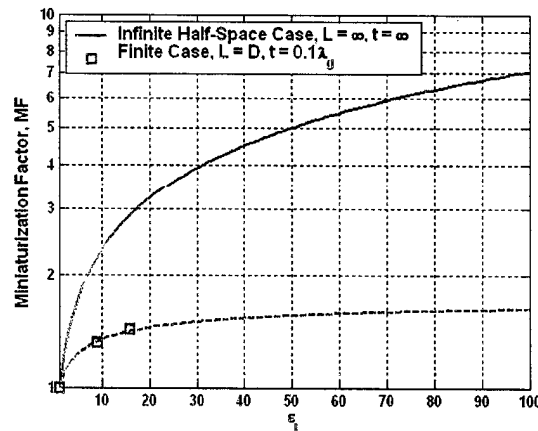
Figure 4.21 Miniaturization factor limitations as a function of dielectric constant for single-sided loading (thickness = $0.1\lambda_g$)

The same approach can be applied to the double-sided loading case and the results are shown in Figure 4.22. In terms of reduction, about 7% more can be achieved as compared to the single-sided loading at the expense of further reduction of the input resistance.
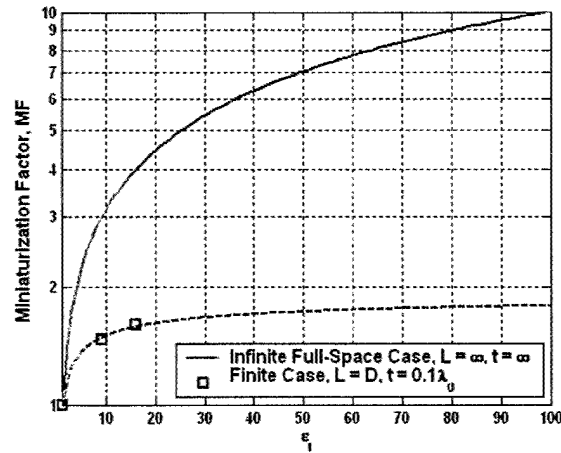
Figure 4.22 Miniaturization factor limitations as a function of dielectric constant for double-sided loading (thickness = 0.1λ$_g$)

In summary, for simple slab loading profiles, the size reduction is limited only by practical loading considerations such as width, profile (thickness), weight and so forth. For such loading profiles it is possible to achieve reductions of 1.54 to 1.8 depending upon the dielectric constant used and, therefore, the amount of impedance reduction that is tolerable. This amount of size reduction is not sufficient to achieve operation down to 30MHz within a 6" or 15" aperture. To achieve operating down to 30 MHz using a 6" and 15" aperture would require miniaturization factors of 11.2 and 4.5 respectively. To realize such reductions we must at least investigate more complex loading profiles and three dimensional antenna designs. These approaches and their concepts are further outlined and discussed in chapter 7.

48

Chapter 5

Antenna Miniaturization Using Reactive Loading

Conventional antenna miniaturization frequently implies dielectric loading. The idea is to miniaturize the wavelength in the antenna structure, thus achieving resonance or movement of the operation point to a lower frequency. Dielectric loading, however, introduces more effects than mere wavelength-miniaturization. First, it modifies the wave impedance inside the antenna, which in turn modifies the antenna impedance. The higher the dielectric constant used, the lower the wave impedance becomes. To compensate this effect one has to either modify the antenna geometry, or to use magnetic material as well. Due to the inhomogeneous nature of the magnetic material and the difficulties associated with its machining, the use of magnetic material greatly complicates the design and analysis. Magnetic material offers limited choices also.

Secondly, dielectric loading introduces an air-dielectric boundary that modifies the radiation behavior. This effect is negligible as long as the electrical thickness is less than a quarter wavelength, but is a dominate factor once the thickness becomes electrically large. Dielectric loading also adds volume and weight.

In this chapter, a novel alternative of antenna miniaturization approach utilizing artificial transmission line (ATL) structure is investigated. The theoretical model and simulation characterization of ATL will be presented. Also, the limit to which the model is valid will then be identified. Subsequently, the artificial transmission line will be applied to antenna geometry and its impact will be examined.
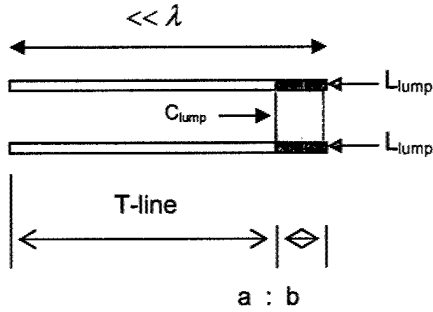
5.1 Artificial Transmission Line (ATL) Concept

For a lossless two-conductor transmission line that propagate in TEM mode, the characteristic impedance and its wave velocity is described as

$$Z_0 = G\sqrt{\frac{\mu}{\varepsilon}} = \sqrt{\frac{L_{eff}}{C_{eff}}}$$

$$v = \frac{1}{\sqrt{\mu\varepsilon}} = \frac{1}{\sqrt{L_{eff}C_{eff}}}$$

where G is geometry factor and L_{eff} and C_{eff} are equivalent inductance and capacitance per unit length. To change the wave velocity or characteristic impedance one needs to adjust L_{eff} or C_{eff} or both. As can be seen in the formula the material loading is one way to achieve this. However, it should also be possible to change the circuit equivalent L_{eff} and C_{eff} by using real circuit elements. The proposed configuration consists of a normal transmission line with repetitive portions replaced by the lumped elements. The geometry of a repetitive segment and a simple weighting function formula predicting L_{eff} and C_{eff} are given below.

$$L_{eff} \approx \frac{a \times L_{T-line} + b \times 2L_{lump}}{a+b}$$

$$C_{eff} \approx \frac{a \times C_{T-line} + b \times C_{lump}}{a+b}$$

This length-based weighting function model assumes that the length of the repetitive segment is short relative to the wavelength. Since both capacitors and inductors are used, it is possible to individually change the characteristic impedance and wave velocity of the transmission line. A set of simulations using HFSS was performed to demonstrate this idea. In this simulator, the artificial transmission line was set up as shown in Figure 5.1.
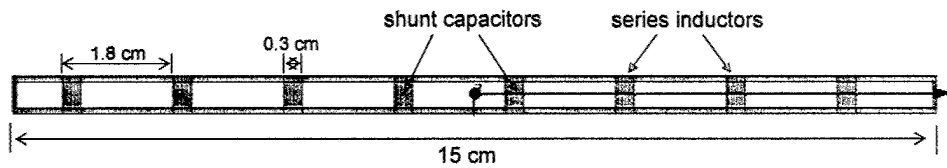
Figure 5.1 Artificial transmission line (ATL) layout.

The capacitor and inductor values were chosen such that the wave velocity on the transmission line is decreased while its characteristic impedance stays the same. Also, the length ratio of the transmission line segment to the lumped element segment was 5:1 and the total

50

repetitive segment length was 1.8 cm. This is about 12 % of the free space wavelength at 1 GHz. Here we define the miniaturization factor, η, as λ_0/λ, where λ_0 is the free space wavelength and λ is the equivalent wavelength on the transmission line. Several cases resulting in a MF of 1.7 to 8.6 were designed and simulated. The phase difference between the two ends of the transmission line as a function of frequency is shown below.
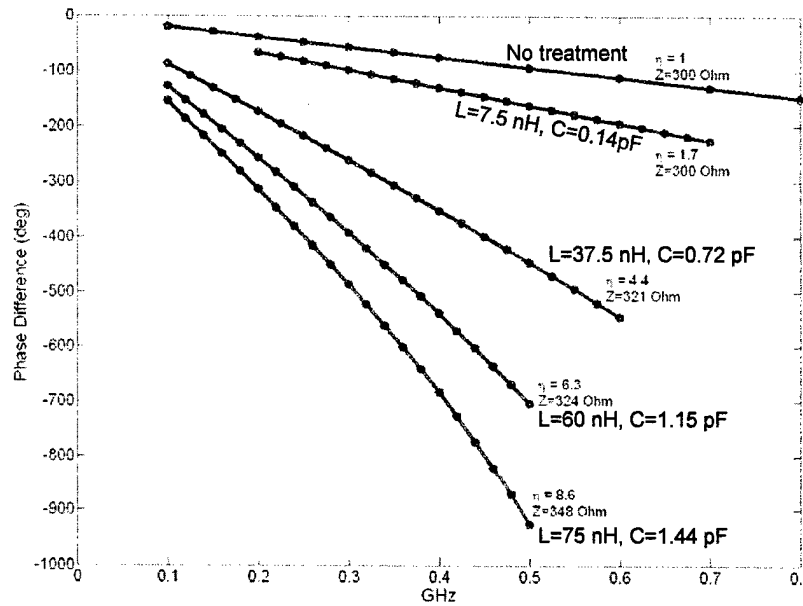
Figure 5.2 Phase difference between the two ends of the ATL as a function of frequency.

The miniaturization of the equivalent wavelength can be clearly observed. It is interesting to note that the cases which have the highest miniaturization factor, 6.3 and 8.6 respectively, demonstrate distinctive nonlinear behavior in the plot. This is obviously due to the fact that the equivalent wavelength at these cases is no longer much greater than the repetitive segment length. For η=8.6 case at 0.5 GHz, the repetitive segment length is 52 % of the equivalent wavelength. At this situation, the breakdown of the weighting function model is understandable. When the equivalent wavelength is comparable to the repetitive segment length, the proposed structure behaves more like a 1-D crystal structure than a uniformed equivalent transmission line. It is necessary to establish a band structure description to accurately explain the nonlinear behavior.

To demonstrate the validity and the limit of the weighting function model, it is useful to observe the detail field distribution on the artificial transmission line. A comparison between the untreated case and η=8.6 case is shown in Figure 5.3.

51
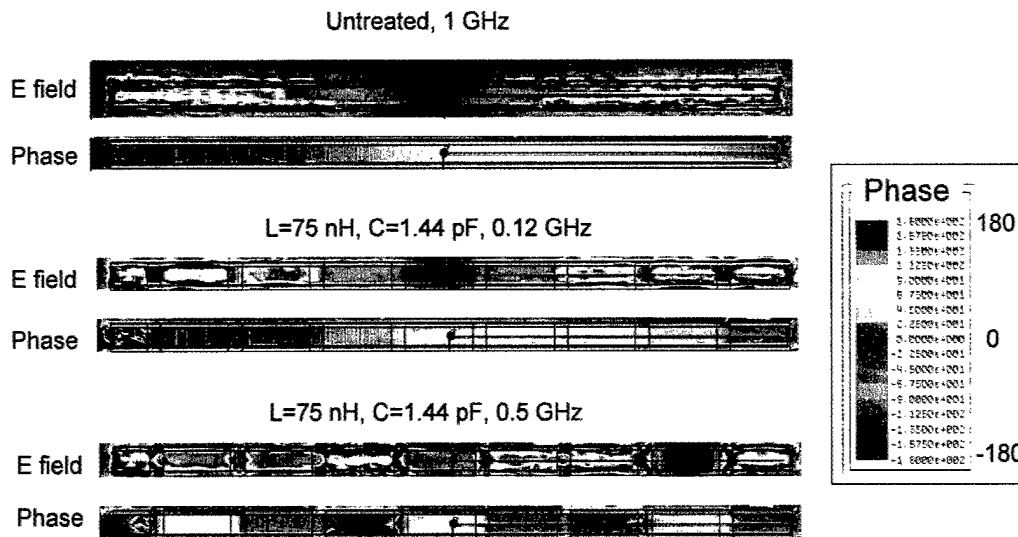
Figure 5.3 ATL field distribution for the untreated transmission line and a treated transmission line.

It can be observed from the first two sets of plot that the lumped elements, though separately distributed, are able to modify the field distribution in an averaged way. Notice also that the artificial transmission line is able to reproduce the field distribution of that of the untreated case at a much lower frequency. Under this situation the equivalent wavelength is still much larger than the repetitive segment length, and the weighting function model is valid. The third set of plots demonstrates the breakdown of the weighting function model. Notice the field variation in this case is very much dependant on the location of the lumped elements, where sudden field variation can be observed. The breakdown of the simple weighting function model doesn't mean that the artificial transmission line ceases to propagate energy. It just means a more detailed model is needed to describe its behavior.

The wave velocity of the artificial transmission line can be calculated from the simulation data, and is shown in Figure 5.4.
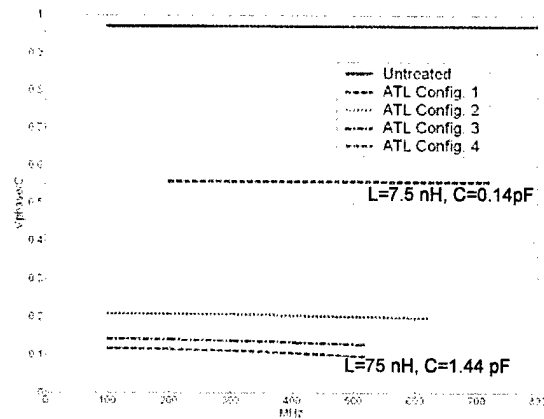
Figure 5.4 Achieved phase velocity of the artificial transmission line.

The slow wave phenomenon demonstrated above, if implemented by using dielectric material, would result in substantial drop of the transmission line characteristic impedance. Instead, the artificial transmission line proposed here is able to maintain a relatively stable impedance value (see Figure 5.5).
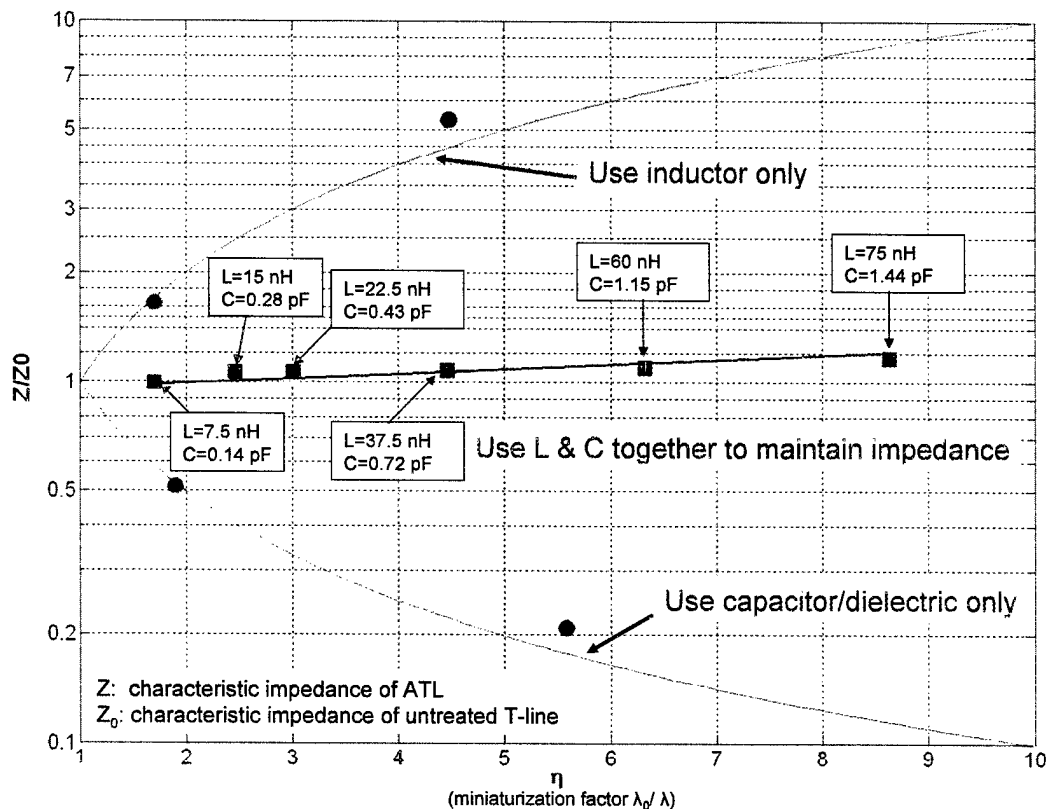
Figure 5.5 Transmission line characteristic impedance as a function of miniaturization.

5.2 Application to Antennas

5.2.1 Narrowband Square Loop Antenna

In this section an artificial transmission line structure is applied to two antennas to examine its miniaturization effect and radiation characteristics. The first antenna geometry studied is a square transmission line loop. The size of the loop is designed for resonance at 1GHz. The geometry of the loop and the field distribution at resonance is shown below.
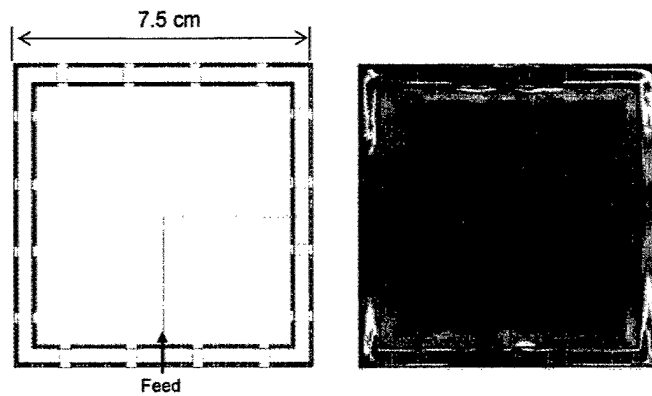
Figure 5.6 Treated square loop antenna (left) and its field distribution at resonance (right).
The transmission line structure without lumped element treatment has a characteristic impedance of 300Ω and our intent is to maintain this impedance by using the appropriate combination of L and C along the line. One untreated case and two treated cases were simulated and broadside realized gain was calculated and is shown in Figure 5.7.
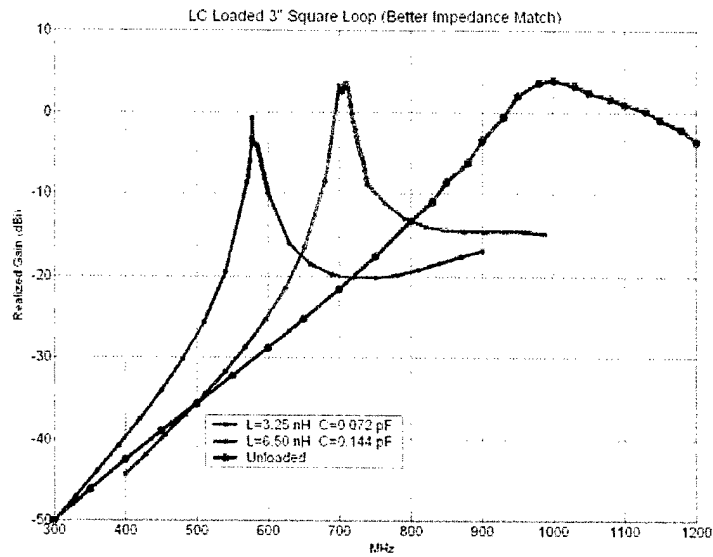
Figure 5.7 Simulated broadside gain for the loaded square loop antenna.

It is apparent from Figure 5.7 that the resonance frequency shifts according to design. However, at the same time, the bandwidth is reduced which is expected for the single mode, resonant type small antenna since the bandwidth for resonant antennas is inversely proportional to the $\sqrt{LC}$. The shifting of the resonant frequency and the change in bandwidth is clearly observed in the impedance plot shown in Figure 5.8.
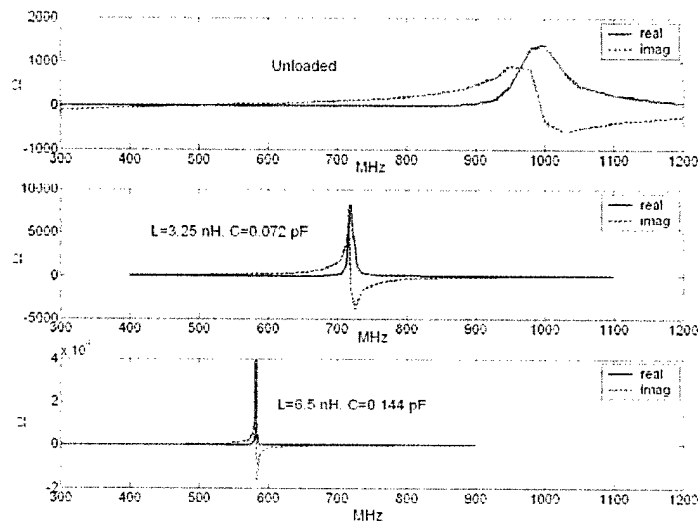
Figure 5.8 Simulated input impedance for the loaded square loop antenna.

The dramatic increase in the real part of the impedance for the miniaturized antennas can be attributed to the electrically small radiation aperture. Also the conductor used in the simulation is

assumed to be perfectly conducting (PEC). The choice of using PEC in the simulation is made to emphasize the mechanism we want to observe. For finite conductivities (as in the practical case) the efficiency loss due to conductor losses must also be considered.

5.2.2 Broadband Spiral Antenna

To demonstrate the miniaturization of a broadband antenna using LC loading a spiral antenna is also implemented and simulated. The two arm Archimedean spiral was terminated with a single resistor that matched the transmission line characteristic impedance. For the artificial transmission line segment, the repetitive segment length is 9mm of which 8mm is ordinary transmission line and 1mm is occupied by the lumped elements. The lumped elements were chosen to miniaturize the wavelength without changing the characteristic impedance. The antenna geometry and the electric field distribution at 1 GHz are demonstrated in Figure 5.9.
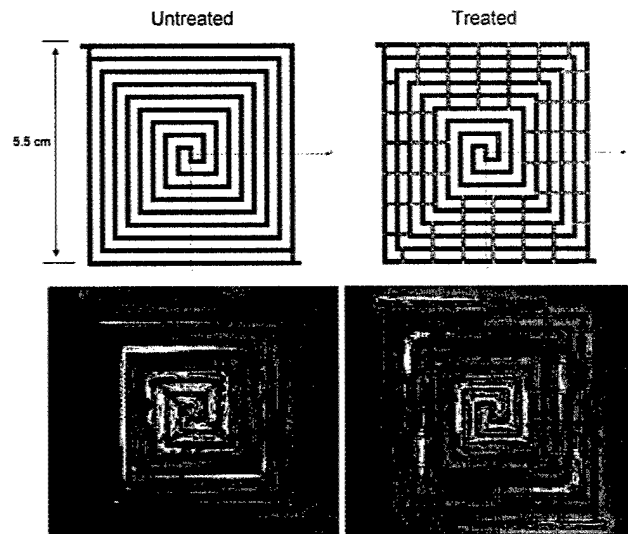
Figure 5.9 Untreated and treated Archimedean spiral and a sample field distribution at 1 GHz.

The realized broadside gain for the two antennas are compared and shown in Figure 5.10. The shifting of the gain curve towards lower frequencies is observed. It is interesting to note, however, that the percentage of frequency shifting in the gain curve does not follow the percentage of wavelength miniaturization. The wavelength on the treated spiral antenna is about 30% of the untreated case, implying a 70% shift in wavelength. However, the gain frequency shift is only about 17% which is four times smaller than the wavelength reduction. We suspect this is due to the fact that while the application of artificial transmission line may miniaturize the

wavelength of the guided wave within the geometry, the antenna eventually has to radiate into free space. Since the 3-D reactive region of the spiral antenna cannot be comprehensively treated with mere lumped element loading, which is basically a 2-D treatment, the resulting miniaturization is limited. A similar observation can be made in chapter 3 when the spiral is loaded with thin dielectric slabs. To a degree, our studies on miniaturization either by dielectric loading or reactive L/C loading allows us to conclude that wavelength miniaturization can be effectively achieved and predicted. However, this wavelength reduction does not translate to a corresponding shift of the gain curve towards lower frequencies. It is our belief that this is due to the 3D nature of the radiated fields around the antenna. Therefore, the 2D miniaturization leads to only partial antenna miniaturization. In the final chapter, we will discuss how we can translate more of the wavelength reduction to antenna miniaturization.
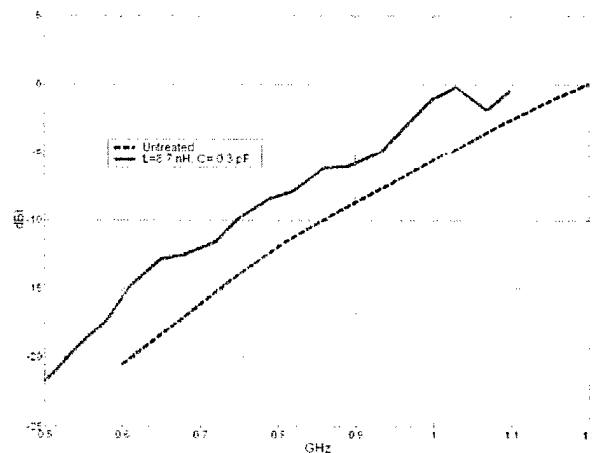
Figure 5.10 Simulated realized gain for the untreated (blue) and treated (red) Archimedean spiral.

Chapter 6

Formal Design Optimization Efforts

6.1 Materials design for improvements in matching and miniaturizations

6.1.1 Motivation

The design challenge is to miniaturize an antenna and still retain its bandwidth with a satisfactory gain performance. Formal design optimization procedures present a high-risk approach to achieve this and for a demonstration we will do this for a SATCOM antenna.

It is well known that use of composite materials provides for greater potential in designing new electromagnetic/RF devices. Therefore, instead of the more traditional approaches to concentrate only on the shape or geometry of the antenna via reactive loading, parasitic coupling and etching, here we focus on both the material substrate/superstrate of the antenna using high-contrast LTCC material and the geometry of an initial random antenna. Our previous studies on metamaterials indicate that properly designed dielectrics or a combination of different materials can lead to designs which have greater bandwidth and small size [8]. Nevertheless, the focus so far has been on narrowband antennas. Here, our goal is to deliver the optimal SATCOM performance in terms of size, gain and impedance matching by optimizing the metamaterial profile of the broadband antenna as well as the shape of the antenna.

The design methods for these devices mainly focus on optimizing the shape and size of the antenna structure rather than its topology and material composition or possibly both. However, a volumetric design of the material composition allows for a greater design possibility. To take full advantage of volumetric variations optimization schemes are used to simultaneously select the best geometric and topological configuration while taking into consideration the

geometry and physical dimensions as well as material composition. Such methods are known as topology optimizations and they are capable of producing novel designs that lead to significant improvements in a device's performance. In terms of the design optimization/solution technique both heuristic and deterministic techniques are used simultaneously to effectively retain inherent advantages of both methods and arrive at a versatile, efficient design methodology which will lead to globally optimum novel designs.

6.1.2 Hybrid Design Optimization Approach

6.1.2.1 Background

In any automated optimum design approach (AOD) the goal is to identify in some automatic process the device structure subject to some prescribed performance. Among existing design methods are size, shape and topology optimization. When compared with more conventional size and shape optimization, where the topology of the device is assumed a priori and remains fixed, topology optimization offers much more degrees of freedom. Consequently, it is reasonable to expect that designs resulting from topology optimization have novel configurations with much higher performance.

As is well known, the solution of design optimization problems is done iteratively. Historically, these iterations were carried out by cut and try operations taking months for each iteration or test. That is, the design process relied on experience and intuition and was impractical. Today, modern optimization theory offers a great variety of automated techniques for solving optimization problems in EM. These can be generally categorized in deterministic and stochastic techniques. Deterministic techniques (e.g. Simplex, Rosenbrock, gradient, quasi-Newton, Newton-Raphson, Sequential Quadratic Programming, Lagrangian Multipliers) seek the minimum point based on the information given by the negative of the gradient (sensitivity) of the objective function. Challenges in their implementation are the requirement to evaluate the gradient of the objective function and issues relating to the algorithm convergence to a global optimum. In contrast, gradient based techniques are mathematically well-behaved and do not involve heuristics which leads to a more efficient solution.

With regard to gradient-free (stochastic methods) optimizers, their utilization has been quite substantial over the 1990's. Popular techniques in this category are simulated annealing (SA) and genetic algorithms (GAs) [9]. For the past several decades, gradient-free methods (a class of optimization methods which do not use derivative information but instead rely only on function values) have been introduced to search for global optima. Gradient-free methods [10], or direct-search methods, are generally robust and particularly effective for problems with a small number of design variables, but typically require fast objective function evaluations for their practical implementation. They are largely independent of the initial design and solution domain. Therefore, global optima are more likely to be found. As can be understood, the gradient-free methods work very well when many local optima exist, whereas gradient-based methods [11, 12] break down in these cases. On the other hand, gradient-free methods are generally slow and require a large number of objective function evaluations to achieve convergence. Hence, they have limited use in problems involving complicated electromagnetic structures where traditional numerical simulations must be used for the objective function computation.

A hybrid optimization technique combining deterministic and heuristic techniques could possibly combine the advantages of both methods and allow for the efficient design of 3D multi-objective designs such as the design of a miniaturized broadband SATCOM antenna with satisfactory gain performance. Therefore, we propose a 2 step design approach based on the combination of a GA and the Density Method to be solved via the SLP. This method is targeted to remove limitations on the geometry and material of the structure to be designed and to arrive at globally optimum novel designs with arbitrary topology and material composition.

Below, we begin by briefly discussing the design methodology and its solution technique via their integration with the FEMA-BRICK solver [13]. We then proceed to present the results of our initial effort to use it to design a 6" antenna with 230-330 MHz bandwidth antenna from scratch.

6.1.2.2 Proposed Approach

The design methodology is based on a two step design algorithm. The initial design step aims to optimize the metallization of the antenna structure subject to prescribed antenna size and material composition. For the solution of the standard optimization approach we will use the

on/off approach via Genetic Algorithms to locate an initial metallization of the antenna subject to given constraints. The second major step focuses on improving the antenna performance by optimizing the volumetric material composition using a topology optimization methodology. The design flowchart is provided in Figure 6.1.
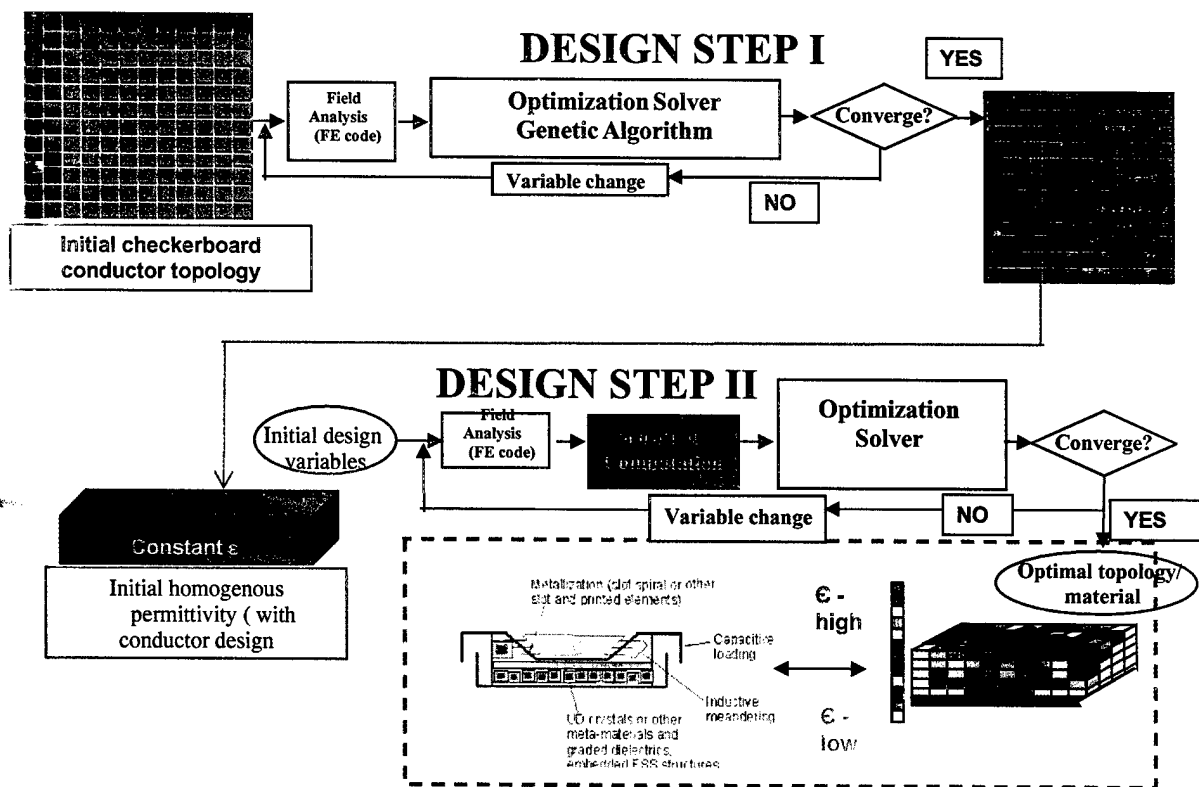
Figure 6.1 Proposed hybrid two step design optimization approach.

For the material design part we will employ the Solid Isotropic Material with Penalization (SIMP) technique [14]. Unlike conventional design methods, SIMP is a topology design method that draws from a broader class of design solutions. Through a simple continuous material model, geometrical and material configurations are effectively designed from 'scratch'. The continuous model allows for a design problem formulation in a non-linear optimization framework using the Finite Element–Boundary Integral method as the computational engine. Sequential Linear Programming (SLP) is then used to solve the optimization problem with sensitivity analysis based on the adjoint variable method for complex variables [8]. The proposed design method allows for inhomogeneous material modeling and design to increase the bandwidth of a fixed size antenna by using a high-contrast LTCC superstrate. It is important to note that the initial design of the second design step corresponds to the optimization result of the

first design step shown in Figure 6.1. This global hybrid design optimization method will allow for multi-objective large scale design problems to arrive at globally optimum designs. There are several different modules involved in the proposed design.

6.1.2.3 Metallization Design via Genetic Algorithms (GA)

GAs are robust, stochastic-based search methods modeled on the concepts of natural selection and evolution, and their underlying process has already been discussed [15, 16]. There are two basic types of operators for GAs. The crossover operator swaps parts of two solutions to generate two new solutions, and the mutation operator randomly changes a small percentage of bits in chromosomes, from 1 to 0 or vice versa. The flowchart for a GA process is shown in Figure 6.2. In the beginning, a desired performance is described and formulated as a fitness function $f(x)$ to be minimized by the GA optimizer, where x is a vector of design variables (e.g. yes or no metallization of each pixel in the design domain, yes or no on the use of available dielectric at certain locations, etc.). If the optimization model contains constraints, they can be included as penalties in the fitness function or encoded directly into the solution strings. Several initial designs coded into binary strings are produced for the first generation either by the user or randomly. For each design, the fitness values are computed using the FEMA-BRICK solver and rated. Good solutions survive and have off-springs, while bad solutions are discontinued. Pairs of good solutions are selected using certain strategies to perform crossover. Mutation is usually allowed with a very small probability to flip some bits from 0 to 1 in the binary string and vice versa, thus providing a way to introduce new designs. This process is repeated until the termination criteria are met. Then the optimal binary string is decoded back into the corresponding design. In GA, local optima are avoided by hyperplane sampling in the Hamming space (i.e., crossovers) plus random perturbations (i.e, mutations).
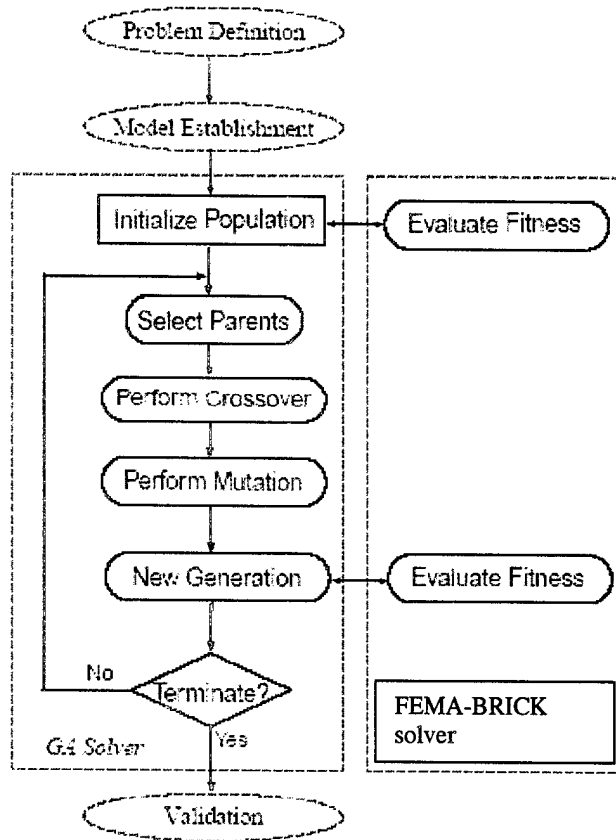
Figure 6.2 General optimization process using GA and FEM solver.

6.1.2.4 Volumetric material design via SIMP and SLP

The essence of SIMP is that it basically assumes some explicit relationship between the so-called normalized density ρ and the actual material property, here the dielectric permittivity $\varepsilon = \varepsilon_0 \varepsilon_r$. The approach has the advantage that a material property is interpolated/graded using a smooth continuous function, which only depends on the material density and almost all possible topologies can be designed within the resolution of the finite element discretization. A suitable interpolation of the dielectric permittivity would be:

$$\rho = (\varepsilon_{\text{int}} - \varepsilon_{air}) / (\varepsilon_{orig} - \varepsilon_{air})^{1/n} \tag{1}$$

where ε_{int} and ε_{orig} are the intermediate and available original (relative) dielectric permittivities of the solid, respectively. The power $1/n$ is an empirical penalization power smaller than $1/2$ for convergence purposes. An important aspect is that this parameterization allows for the formulation of the problem in a general non-linear optimization framework. The goal is to arrive at the optimum distribution of material (densities) such that a specific performance merit of a device is optimized subject to certain design constraints. For this purpose, the design volume is divided into design cells/finite elements to introduce a full volumetric design space. The material property of each design cell is controlled simultaneously in each iteration step and updated by following a mathematical algorithm to reach a final design. From this viewpoint, a device is represented by material properties at every point in space via a single density variable.

A suitable optimization model for the SATCOM antenna corresponds to the minimization of the objective function:

$$f(\rho) = \min\left[\max(|s_{11}|_j) \right] \quad j = 1,...N_{freq} \tag{2}$$

subject to a material volume constraint:

$$\sum_{i=1}^{NFE} \rho_i \cdot V_i \leq V^* \tag{3}$$

and side constraints (0/1) for each density variable. Minimization of the highest return loss among sampled frequency points N_{freq} is known to maximize the return loss (S11) bandwidth and the volume constraint basically limits the available amount of material. The design problem is easily recognized as a general non-linear optimization problem with usually several thousand variables/FEs. This makes the use of gradient-based optimization techniques a must for the optimization process. Due to its well-known efficiency and reliability, we specifically chose the Sequential Linear Programming (SLP) method employing the DSPLP package in the SLATEC library [17]. The essence of the SLP routine is to replace the objective function and constraints by their linear approximations at each iteration. Updates of the design variables are pursued thru the use of gradient information obtained via the adjoint variable method [18], an efficient method that permits full interface with the FEMA-BRICK electromagnetic solver. We remark that this is an exact analysis based on the solution of the adjoint problem. The sensitivity analysis is a crucial part of the design loop since it allows the integration of the solver with the SLP optimizer. Details on the sensitivity analysis are given in [8] for the return loss and are derived and implemented similarly for the gain measure.

6.1.3 Initial Design Efforts

In this section, we present our initial efforts for the design of a 6" SATCOM antenna to satisfy the 230-330MHz bandwidth requirement from scratch. The initially chosen antenna structure is shown in Figure 6.3. It corresponds to a horizontally fed strip antenna buried within a 6cm thick cavity backed antenna. The design region corresponds to the discretized metallization layer initially composed of that horizontally fed strip conductor sandwiched between $\varepsilon=37$ dielectrics each of 1cm thickness. The cavity below the dielectric is 3cm thick. The optimization will seek for the metallization distribution that will improve the bandwidth performance of the initially random antenna structure that happens to have no resonance within the desired frequency band. Following the algorithm for the 1st design step described above and updating the metallization pattern via a micro-GA, the design resulted in a double resonance return loss behavior as shown in Figure 6.4. Convergence to the metallization pattern shown in Figure 6.4 where a conducting element is denoted with a red cell was achieved in 174 generations for a population of 5 individuals and a frequency range (230 MHz-330MHz) sampled with 51 frequency points. Obviously the corresponding return loss behavior does not satisfy the SATCOM antenna requirements but represents a significant improvement over the chosen initial design.

As described earlier, the subsequent design step will be to tune the antenna performance with the resulting metallization pattern as the initial design as shown in Figure 6.5. That is, for the second design step the metallization pattern and size of the structure will remain fixed and the resulting metallization will be fed into the subsequent design algorithm to search for the optimum material distribution to improve the bandwidth performance. By updating the material design cells via the SIMP model and the SLP routine as discussed earlier, the design arrived at a -4dB flat return loss response in only 19 iterations. The initial and resulting optimized return loss behaviors are compared as shown in Figure 6.6. It is important to note that the variables of the design problem are the dielectric constants of each finite brick element and the optimized material distribution corresponds to the material variation of different layers above and below the metallization pattern. This material distribution is a high-contrast volumetric material composite composed of 3 layers each of 1cm thickness as shown in Figure 6.7. At this point we did not pursue the fabrication of this layer high-contrast composite since we need to improve the return loss response even further and possible push down the -4dB level to -10dB.

Initial Design Parameters

Top View (Horizontally fed Metal) of Conductor Design Space with Fixed Metal Strip

ε = 37   2 cm

Metallization

ε = 37   1 cm

ε = 1   3 cm

Side View

15 cm

15 cm

Fixed design parameters: Size, Feed, ε and Metal Strip at Feed

Design Variable: ▮ Metal ▮ No Metal
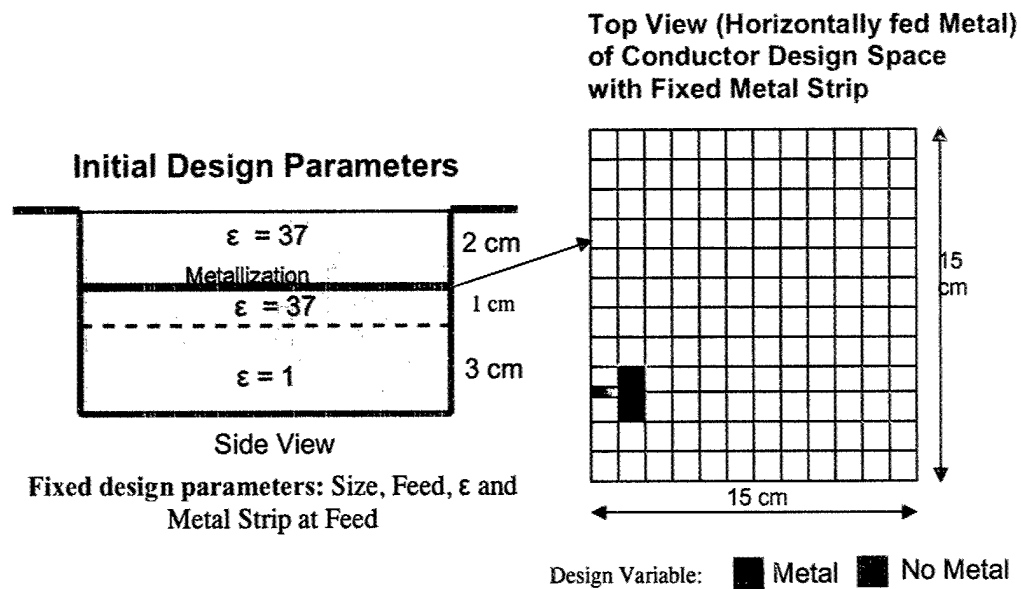
Figure 6.3 Initial antenna structure of 1st design step: Horizontally fed strip antenna with fixed cavity size and material composition. Design variables correspond to on/off (1/0) conductor metallization pattern.

15cm

15 cm

Return loss (dB)

0.2   0.25   0.3

Frequency (GHz)

▮ Metal   ▮ No Metal
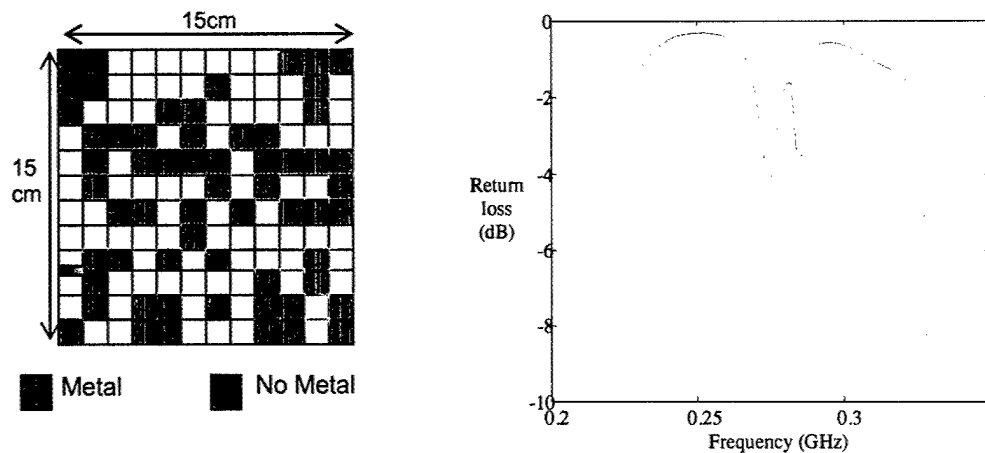
Optimization Tool: Micro Genetic Algorithm
Population: 5
Generation:174
Objective function: min(max(s11))->Max Bandwidth
Frequency Range: 0.23-0.33 (51 frequency points)

Figure 6.4 Resulting metallization pattern of 1st design step via micro-Genetic algorithm and corresponding return loss behavior.

66

Fixed Conductor Topology:
Previous Design Result

Initial Design Parameters

Fixed design parameters: Size, Feed,
Conductor Topology

Design Variable: ε within substrate 1
superstrate 1 and superstrate 2 (initially ε=37)
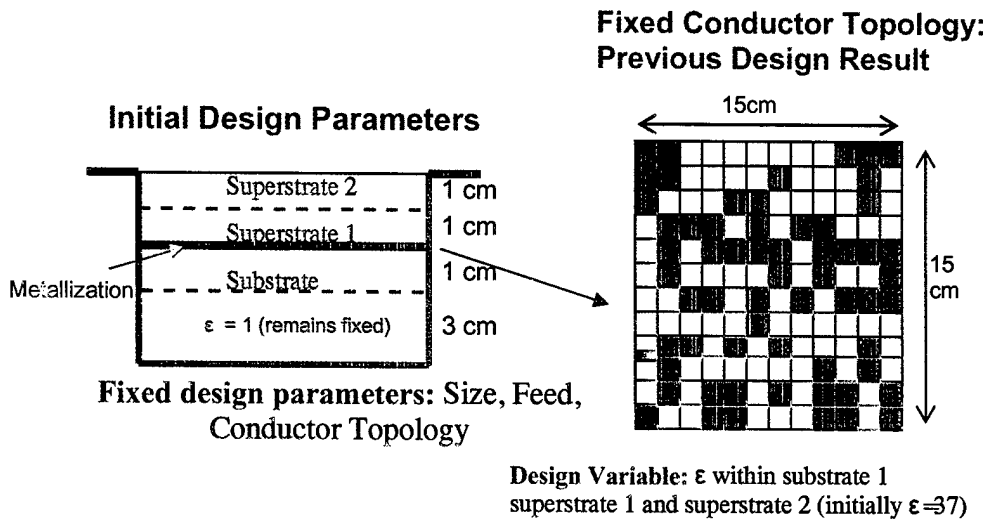
Figure 6.5 Initial antenna structure of 2ⁿᵈ design step: Horizontally fed metallization pattern with fixed cavity size and air cavity. Design variables correspond to volumetric cell's ε values within superstrate and substrate.

Initial vs. optimum material design and return loss
performance with fixed metallization layer
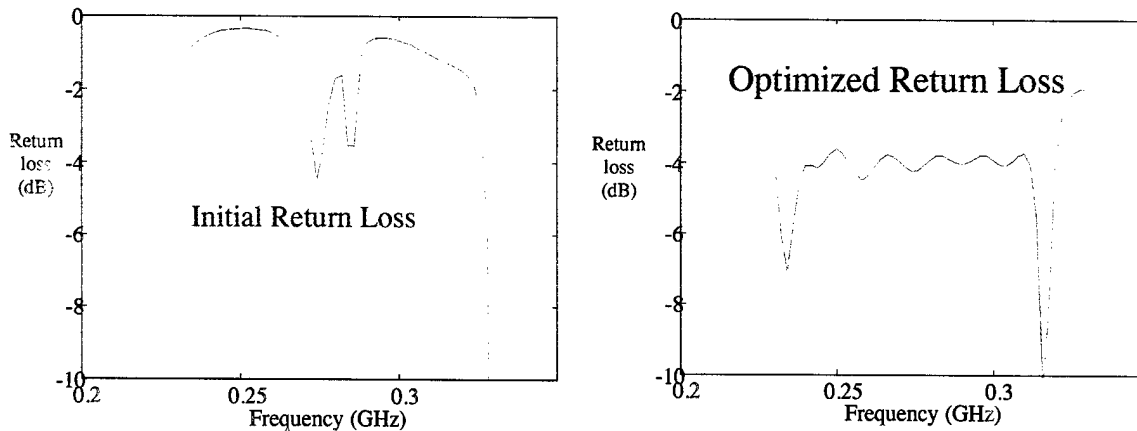
Optimization Tool: Density Method with Sequential Linear Programming
Iteration Number: 19,
Objective function: min(max(s11))->Max Bandwidth
Frequency Range: 0.23-0.33 (51 frequency points)

Figure 6.6 Initial and optimized return loss performance of 2ⁿᵈ design step of material optimization via Density Method and SLP.

67

Optimum material distribution across each layer
via Density Method and integrated smoothing & filtering algorithm

Figure 6.7 Resulting material composition of 2nd design step via Density Method and SLP across each layer of superstrate and substrate region.
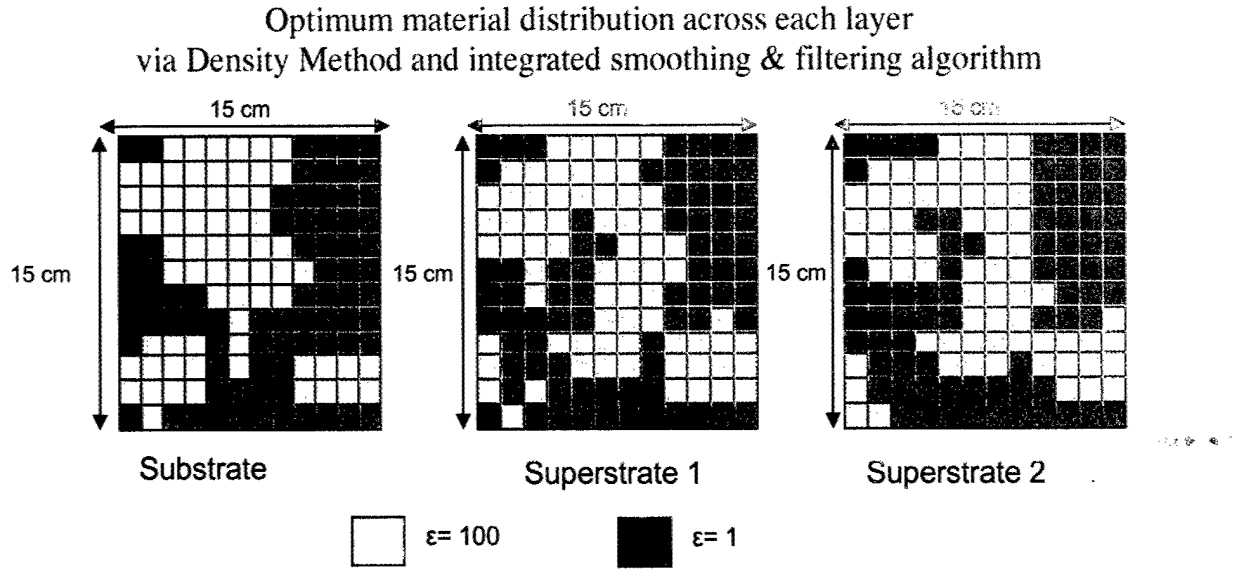
6.1.4 Current and Future Work

Having confidence in the design methodology and promising initial trials we are currently exploring ways to tune the sandwich design with high contrast ceramics to improve the bandwidth response. Possible areas for improvement are:

- *Feeding mechanism*: A probe or microstrip aperture coupling presents additional advantages and will be explored.

- *Multi-layer conductors*: Increasing the number of conducting layers will allow to induce parasitic coupling. Parasitic coupling with proper feeding and material loading offers advantages over single layer metallization to increase the bandwidth behavior further.

- *Multi-layer high-contrast material variation*: Increasing the number of layers within the volumetric cavity of the antenna will increase the design degrees of freedom and possibly increase the bandwidth performance. Naturally, there is a tradeoff between increased CPU requirements and fabrication challenges vs. increased design freedom to achieve better bandwidth response.

68

- *Different material constituents*: Different material combinations are available for our use as high temperature cofiring ceramic powders and may be used to satisfy the SATCOM requirements. Actually, more than only 2 shades of material may achieve a smoother transition at the material and layer interfaces and may result in an improved antenna performance.

- *Design Methodology*: Mix-match of design methodologies such as metallization design via density method and material design via GA might improve the performance of the antenna at the expense of higher CPU and convergence issues.

It is also noted that above listed efforts will result in a different design optimization problem than in our initial efforts and present the potential of changing the results drastically. This change is anticipated due to an altered design region and corresponding different design variables. Our future work plan is based on implementing the gain measure to the optimization model and redesigning the final "best" design subject to both the bandwidth and gain criteria. Important in this process will be the integration of the already developed gain sensitivity module into a design problem with generalized permittivity values accounting for imaginary lossy parts. Another aspect will be the implementation of advanced solution techniques (parallel processing of hybrid techniques and advanced material models) to improve the convergence and CPU requirements for a much larger scale problem. An improved feed model which captures the current variation in a high epsilon thick substrate is another important future topic.

Chapter 7

Future Work

In chapter 4 it was shown that for practical loading configurations only a 35-44% reduction is possible from simple loading profiles. To achieve reductions greater than 50% more complex material loading profiles and/or a 3D antenna design is needed to more effectively load the antenna fields. These approaches are outlined in section 7.1 with each sub section focusing on a particular approach.

In addition to improving the miniaturization it is also important to improve the efficiency of the spiral by exploring the possibilities of a loss-less termination. Future plans for such a termination method are also discussed in section 7.2.

7.1 Concepts for Improved Miniaturization

7.1.1 Shaped Dielectric Layers for Planar Spiral

To achieve reductions greater than 50% using practical loading configurations, the antenna fields must be confined closer to the antenna so that they can be loaded more effectively. Figure 7.1 shows what the typical field lines may look like (left) for the planar spiral and what the desired field lines should look like (right) for better miniaturization. It is evident from this figure that the field lines on the right are confined closer to the spiral and would therefore be easier to load using a slab of reasonable thickness. A possible tactic to confine the fields closer to the spiral would be to use shaped dielectric layers with varying ε_r to control the fields as shown in Figure 7.2. The idea is to use the material shape and varying dielectric constant to force the expanding spherical wave to become more elliptical. However, such a design would be complicated since it will involve determining the proper dielectric constants of each layer, the layer thickness and its shape. Fabricating the dielectric layers would also be another issue.
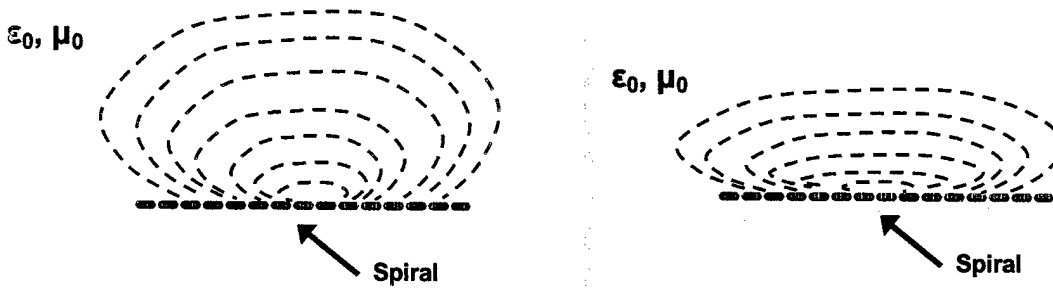
70

Figure 7.1 Left: typical field lines of spiral. Right: desired field lines of spiral.
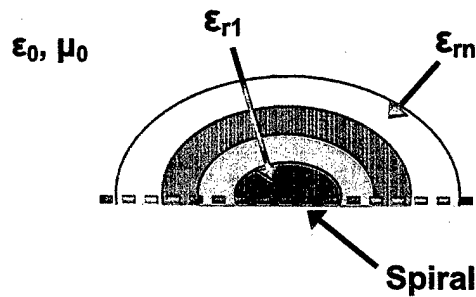

Figure 7.2 Material profile concept for improved miniaturization.

7.1.2 Three-Dimensional Spiral Antenna Design

We know that more effective loading of the near zone fields will result in greater size reduction. The issue with the planar spiral is that at low frequencies the fields extend outside the diameter of the spiral making it difficult to load in a practical manner. If the planar structure is the reason for this, then one way to better load the near fields is to make the spiral non-planar. The concept is to alter the planar spiral shape such that low frequency fields can be confined closer to the antenna aperture without negatively impacting the performance. Thus, they can be loaded more efficiently using practical loading configurations. This concept is illustrated in Figure 7.3 and shows how the fields around the antenna are now more closely confined in the concave portion of the geometry. The extent to which the 3D design can confine the low frequency components with this volume of space is unknown at this time. Furthermore, the 3D design may affect the performance of the spiral in yet a unknown manner.
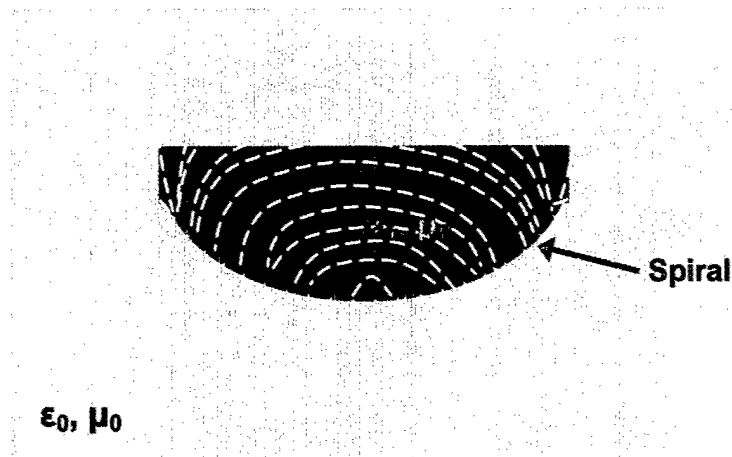
71

Spiral

ε_0, μ_0

Figure 7.3 Illustration of the 3D spiral design concept for improved miniaturization.

7.2 Concept for Improved Arm Termination

For the spiral antenna, a decrease in the phase velocity is always associated with a decrease in the attenuation of the traveling wave through the 1λ region. Since material loading reduces the phase velocity, there is also a corresponding reduction in this attenuation. Therefore, more energy is bound to the spiral and will eventually reach the termination or may radiate from higher order regions (3λ, 5λ, etc.). It is therefore understood that if the arm is terminated using resistors then there may be a significant reduction in antenna efficiency. If the arm is not terminated, then the antenna efficiency will improve but the reflections from the end of the arm will travel back to the feed region and cause oscillations in the input impedance and higher cross-polarization. Therefore, a lossless termination method is an ideal solution since it will prevent reflections while, at the same time, maintain antenna efficiency. One possible way to implement this lossless termination is to modify the antenna such that the current essentially circulates throughout the antenna structure without reflecting.

The idea is to allow the current to pass through the 1λ region as many times as possible and each time through it will be attenuated more and more. The challenge to accomplishing this is to do it in a way that the current is always entering the 1λ region in the same direction. Thus, cross-polarization issues are negated.

One approach is to use two stacked spirals with one of the spirals being a mirror image of the other so that their combined radiation does not cancel one another when placed in the stacked configuration. One of the spirals (A) will be fed in the usual manner. The other spiral B will be

72

fed by connecting the ends of spiral A to the ends of the arms of spiral B. Spiral B will then be connected to the feed region of spiral A through a pair of diodes which will force the current to flow in only one direction throughout the structure. That is the current will flow outwards from the feed region of spiral A to the connection point of the stacked spirals. The current will then flow inwards on spiral B (which is wound with the opposite sense of A) to its center where it will pass through the diodes and re-enter spiral A. This creates a circulating structure on which the current can flow and be attenuated by radiation and ohmic loss each time it passes through the 1λ region of spiral A or B. This structure is illustrated in Figure 7.4 where the red spiral corresponds to spiral A and the blue spiral to spiral B.
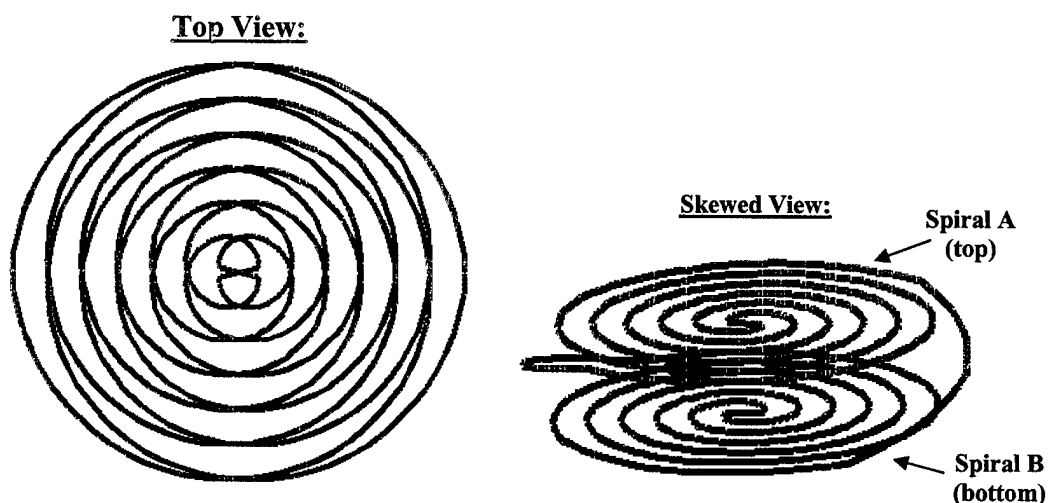
Top View:

Figure 7.4 Illustration of the stacked Archimedean spiral concept for improved termination.

Bibliography

[1]   R. C. Johnson, *Antenna Engineering Handbook*, 3rd Edition, McGraw-Hill , Inc., New York, 1993, chap. 14.

[2]   D.S. Filipovic, J.L. Volakis, "Broadband meanderline slot spiral antenna," *IEE Proceedings. Microwaves, Antennas and Propagation*, Vol. 149, Issue 2, pp. 98 -105, April, 2002.

[3]   M.W. Nurnberger and J.L. Volakis, "Extremely Broadband Slot Spiral Antennas with shallow reflecting cavities", *Electromagnetics*, Vol 20, No. 4, pp. 357-376.

[4]   John L. Volakis, Arindam Chatterjee and Leo C. Kempel, "*Finite Element Method Electromagnetics : Antennas, Microwave Circuits, and Scattering Applications*", John Wiley & Sons, 01 June, 1998.

[5]   J.M. Jin and J.L. Volakis, "A Finite Element-Boundary Integral Formulation for Scattering by Three-Dimensional Cavity-Backed Apertures," *IEEE Trans. Antennas and Propagat..*, AP-39, pp.97-104, January 1991.

[6]   T. Ozdemir, J.L. Volakis and M.W. Nurnberger, "Analysis of Thin Multioctave Cavity-backed Slot Spiral Antennas," *IEE Proceedings-Microwave, Antennas and Propagation*, Vol.146, pp. 447-454, December 1999.

[7]   Rick W. Kindt, John L. Volakis, "The Array Decomposition-Fast Multipole Method for Finite Array Analysis," *Radio Science*, Vol. 39, No. 2, 2004.

[8]   G. Kiziltas, D. Psychoudakis, J. L. Volakis and N. Kikuchi, "Topology design optimization of dielectric substrates for bandwidth improvement of a patch antenna," *IEEE Transactions on Antennas and Propagation,* Vol. 51, No.10, pp. 2732 – 2743, Oct. 2003

[9]   L. Davis, *Genetic Algorithms and Simulated Annealing*. London: Pitman, 1987.

[10]   R. Horst, P.M. Pardalos, and N.V. Thoai, Introduction to Global Optimization, Vol. 3 of Nonconvex Optimization and Its Applications, Kluwer Academic Publishers, Dordrecht, 1995.

[11]   S.S. Rao, Engineering Optimization: Theory and Practice, Wiley, New York, 3rd edition, 1996.

[12]   P.Y. Papalambros and D.J. Wilde, Principles of Optimal Design: Modeling and Computation, Cambridge University Press, New York, 2nd edition, 2000.

[13]   J. Volakis, T. Ozdemir, and J. Gong, "Hybrid finite-element methodologies for antennas and scattering," *IEEE Transactions on Antennas and Propagation,* Vol. 45, No. 3, pp. 493-507, March 1997.

[14]   M. P. Bendsoe, "Optimal shape design as a material distribution problem," *Structural Optimization*, Vol. 1, pp. 193-202, 1989.

[15]   R.L. Haupt, "Introduction to genetic algorithms for electromagnetics," *IEEE Antennas and Propagation Magazine*, Vol. 37, No. 2, pp. 7-15, Apr. 1995.

[16]   J.M. Johnson and Y. Rahmat-Samii, "Genetic algorithms in engineering electromagnetics," *IEEE Antennas and Propagation Magazine*, pp. 7-25, Aug.1997.

[17]   R. Hanson and K. Hiebert, "A sparse linear programming subprogram," *Technical Report SAND81-0297*, Sandia National Lab., 1981.

[18]   D. N. Dyck, D. A. Lowther and E. M. Freeman, "A method of Computing the Sensitivity in Electromagnetic Quantities to changes in Materials and Sources," *IEEE Trans. on Magnetics*, Vol. 30, No. 5, Sept. 1994.